AFIT/GSO/ENG/91D-17

A TOPOGRAPHICAL ANALYSIS OF THE HUMAN ELECTROENCEPHALOGRAM FOR PATTERNS IN THE DEVELOPMENT OF MOTION SICKNESS

THESIS

George S. Vogen, Captain, USAF

AFIT/GSO/ENG/91D-17

REPORT DOCUMENTATION PAGE

Form Approved
OMB No 0704-0188

1. AGENCY USE ONLY (Leave blank)	2. REPORT DATE	3. REPORT TYPE AND DATES COVERED
	December 1991	Master's Thesis

4. TITLE AND SUBTITLE

A Topographical Analysis of the Human Electroencephalogram for Patterns in the Development of Motion Sickness

5. FUNDING NUMBERS

6. AUTHOR(S)

George S. Vogen, Captain, USAF

7. PERFORMING ORGANIZATION NAME(S) AND ADDRESS(ES)

Air Force Institute of Technology, WPAFB OH 45433-6583

8. PERFORMING ORGANIZATION REPORT NUMBER

AFIT/GSO/ENG/91D-17

9. SPONSORING / MONITORING AGENCY NAME(S) AND ADDRESS(ES)

10. SPONSORING MONITORING AGENCY REPORT NUMBER

11. SUPPLEMENTARY NOTES

12a. DISTRIBUTION / AVAILABILITY STATEMENT

Approved for Public Release; Distribution Unlimited

12b. DISTRIBUTION CODE

13. ABSTRACT *(Maximum 200 words)*

A topographical analysis was performed on 12 electroencephalograms (EEGs) collected from 10 volunteers who experienced motion sickness through cross-coupled Coriolis stimulation. Seven males and three females participated in the research conducted at the Air Force Institute of Technology, Wright-Patterson AFB. Two male volunteers participated in double-blind placebo/phenytoin trials. Static brain maps and dynamic EEGs which focused on delta (below 3 Hz) activity during the development of motion sickness revealed a seizure-like propagation pattern. With initial symptoms, a clear left parietal focus was seen in all records. A less dominant left fronto-temporal focus was present in 11 of the 12 records. As symptoms grew there was a contralateral spread (possibly occipitally) to the right temporal region. A steady increase in power was noticeable during the evolution of motion sickness. The 2 phenytoin trials showed less overall power when compared to their respective placebo trials. The report of this seizure-like propagation pattern during motion sickness is believed to be the first of its kind.

14. SUBJECT TERMS

motion sickness, electroencephalography, seizures, convulsive disorders, topographic brain mapping, space adaptation syndrome, epilepsy, anticonvulsants, brain, motion sickness drugs, hydantoins, coriolis effect, physiological effects

15. NUMBER OF PAGES

84

16. PRICE CODE

17. SECURITY CLASSIFICATION OF REPORT	18. SECURITY CLASSIFICATION OF THIS PAGE	19. SECURITY CLASSIFICATION OF ABSTRACT	20. LIMITATION OF ABSTRACT
Unclassified	Unclassified	Unclassified	UL

THESIS APPROVAL

STUDENT: Captain George S. Vogen CLASS: GSO - 91D

THESIS TITLE: A Topographical Analysis of the Human Electroencephalogram for Patterns in the Development of Motion Sickness

DEFENSE DATE: 25 November 1991

GRADE:

COMMITTEE:	NAME/DEPARTMENT	SIGNATURE
Advisor	Dr. Matthew Kabrisky/ENG	
ENS Rep.	Major Thomas S. Kelso/ENS	Thomas Sean Kelso
Reader	Major Steven K. Rogers/ENG	Steven K Rogers (for)

AFIT/GSO/ENG/91D-17

A TOPOGRAPHICAL ANALYSIS OF THE HUMAN ELECTROENCEPHALOGRAM FOR PATTERNS IN THE DEVELOPMENT OF MOTION SICKNESS

THESIS

Presented to the Faculty of the School of Engineering
of the Air Force Institute of Technology
Air University
In Partial Fulfillment of the
Requirements for the Degree of
Master of Science in Space Operations

George S. Vogen, B.S.
Captain, USAF

December 1991

Preface

The purpose of this research was to search for a propagation pattern of electrical activity in the human brain during the development of motion sickness. The discovery of this pattern, through a topographic spectral analysis of the electroencephalogram, should provide a deeper understanding of motion sickness, support further research into its seizure-like similarities, and encourage further investigations in the use of anticonvulsants for preventing motion sickness.

Throughout my research a great number of people are owed my gratitude for making this research possible. Most important are the numerous volunteers who motivated by science, adventure, or maybe dementia participated in the motion sickness experiments to provide the data used in this and related research. The thesis work of Capt. Todd Banducci which set the foundation for my research is also noted. Collection of this data would not have been possible without the help of Dr. William Chelen who, as an electrical engineer and physician, provided me his technical and medical expertise when questions surfaced. I thank my advisor, Dr. Matthew Kabrisky, and my reader, Major Steven K. Rogers, for introducing me to what they call the church of electrical engineering, for fascinating me in the mysteries of the brain, and for having the faith in me to pursue this research. I also thank Major Thomas S. Kelso, my representative from the Operational Sciences department, for his encouragement and for his interest my research.

Finally, I would like to dedicate this thesis to my mother and the memory of my father whose love and guidance through the years has allowed me to appreciate the value of hard work and an education.

It is the customary fate of new truths to begin as heresies and to end as superstitions

-- T. H. Huxley, *The Coming of Age of "The Origin of Species"*

George S. Vogen

Table of Contents

List of Figures

List of Tables

Abstract

A topographical analysis was performed on 12 electroencephalograms (EEGs) collected from 10 volunteers who experienced motion sickness through cross-coupled Coriolis stimulation. Seven males and three females participated in the research conducted at the Air Force Institute of Technology, Wright-Patterson AFB. Two male volunteers participated in double-blind placebo/phenytoin trials. Static brain maps and dynamic EEGs which focused on delta (below 3 Hz) activity during the development of motion sickness revealed a seizure-like propagation pattern. With initial symptoms, a clear left parietal focus was seen in all records. A less dominant left fronto-temporal focus was present in 11 of the 12 records. As symptoms grew there was a contralateral spread (possibly occipitally) to the right temporal region. A steady increase in power was noticeable during the evolution of motion sickness. The 2 phenytoin trials showed less overall power when compared to their respective placebo trials. The report of this seizure-like propagation pattern during motion sickness is believed to be the first of its kind.

I. Introduction

1 Background

Motion sickness, a malady characterized by headache, pallor, cold sweating, malaise, lethargy, nausea, and vomiting, has probably afflicted man since the earliest days of transportation (9: 1185; 12: 468-9; 49: 2). In addition to the relative discomfort experienced by those afflicted with motion sickness, there exists the potential of motion sickness to create operationally significant hazards or liabilities to those traveling by air, land, sea, or space (2: 1-7; 4: 470-1; 49: 28-37).

The growing interest toward increasing a manned presence in space has drawn particular attention to the area of space motion sickness (SMS) or perhaps, more properly, space adaptation syndrome (SAS). SMS affected 67 percent of the astronauts during the first 24 shuttle flights and has been called "the most clinically significant medical phenomenon during the first several days of spaceflight" (9: 1185). The post-Challenger and the Soviet manned experiences with SMS are equally alarming (10; 27: 36.1). As a result, research continues in trying to understand the cause of motion sickness and to find possible preventions or cures.

Treatment and prevention of motion sickness has primarily fallen into three areas: desensitization, biofeedback, and drug therapy. Desensitization involves repeated exposures to the motion sickness stimulus until the individual adapts to the stimulus (12: 488-9; 49: 233-6). Biofeedback primarily consists of obtaining information on the physiologic signs of motion sickness and applying various relaxation techniques to control these signs (32: 1153, 34: 36).

Each of the above prevention techniques has had varying levels of success, as well as certain drawbacks. Desensitization requires repeated exposures to motion sickness; biofeedback requires subject cooperation, concentration, time, and medical oversight; and drug therapy may involve undesired side-effects (9:1188; 12:487-93; 32:1157; 49:219-24, 233-6).

In 1982, the Air Force Institute of Technology (AFIT) started it's research in motion sickness by developing a system to obtain physiologic measurements during the development of motion sickness. This research soon evolved into the area of drug therapy when the appearance of high-voltage, low-frequency (below 3 Hz) electrical signals in the brain (electroencephalogram or EEG), similar to those sometimes seen in partial seizures, were detected (5: 2). This similarity and others have led to the testing of the anticonvulsant drug, phenytoin, which has produced positive results, as this author can attest (6: 1022-4). In addition, similar research in using phenytoin as a motion sickness treatment is being conducted by the Soviets and is considered very promising (37: 92).

Combining the hypothesis that motion sickness is similar to a partial seizure (a form of epilepsy) with the fact that the frequency analysis of an EEG of an epileptic patient is useful in understanding and treating epilepsy leads to the idea which follows (36; 41; 43: 685-706; 44; 45; 46). Analysis of the EEG may provide a deeper understanding of the neurological basis of motion sickness and provide significant information for the prevention of motion sickness.

2 Problem Statement

2.1 Primary Objective

The purpose of this research is to analyze the human electroencephalogram, through the use of brain topographical maps, to determine if a propagation pattern in the evolution of motion sickness exists.

2.2 Sub-Objectives

The following sub-objectives, associated with the primary objective, will also be considered during the course of this study:

1) Provide a deeper understanding of motion sickness;

2) Find a feature suitable for recognizing patterns in the EEG development of motion sickness;

3) Investigate whether there is any discernable difference between the EEGs of phenytoin-treated and untreated subjects;

4) Consider whether continued research in the use of anticonvulsant medications for preventing motion sickness offers further promise.

3. Scope

The EEG data used in the course of this research was collected at the AFIT Motion Sickness Lab from ten healthy normal volunteers from 26 to 41 years of age (methods discussed in Chapter IV). Five male and three female active duty military personnel volunteered to provide EEG data without treatment of phenytoin (females were prohibited from phenytoin treatment since it is a teratogenic). Two male active duty military personnel participated in double-blind placebo/phenytoin experiments. Therefore, a total of 12 EEG records were available for analysis. Four records contained motion sickness data up to a point of nausea or severe nausea. The final eight records contained data through the point of emesis. The analysis of each EEG record was limited to use of a computerized brain topography system, although the raw analog EEG data was used as a means to validate results.

4 Assumptions

The following key assumptions were made in conducting this research:

1. All the equipment used in the collection of EEG data was functioning as designed.

2. A propagation pattern exists but a good feature or a suitable characteristic must be used to make the pattern recognizable. Therefore, the problem is a pattern recognition one.

3. The frequency range below 3 hertz (delta) is key to finding the pattern.

4. The physiological changes which occur during the evolution of motion sickness correlate to the subjective state-of-health reports of the subjects and, therefore, these reports are reasonably accurate (3; 16).

5. The EEG data subject to analysis was relatively artifact free and any artifact which was undetected was insignificant to the results.

6. Subjects are equally susceptible from one trial to the next and, therefore, no adaptation occurs (54: 566, 568-572).

7. The results are representative of the results that would be obtained from the healthy normal population.

II Matters of Importance

The purpose of this research is to perform a signal analysis of the electrical signals generated by the brain. However, this problem encompasses a variety of specialized areas, each of which should be generally understood before proceeding. Chapter II is therefore written, with the nonspecialized reader in mind, to provide a basic background of the concepts and terminology used in this research. This chapter will not, however, go into great detail on the general structure of the brain or the characteristics of motion sickness. Numerous publications in these areas are available for the interested reader (12; 21; 26; 38; 39; 49; 50; 51).

A brief review of how electrical signals are generated in the brain will be the first matter of discussion. Second, a quick look at the role the vestibular system plays in contributing to motion sickness is given. Next, a slightly more detailed look into the characteristics, problems, and considerations of electroencephalography and the EEG is accomplished. Fourth, due to the similarities between motion sickness and simple partial seizures, some characteristics of the partial seizure and how a seizure may affect the EEG are introduced. Finally, the role phenytoin plays in inhibiting seizure-like activity is provided. Following this discussion in Chapter II, a review of methods used in performing a topographic analysis of the EEG will be conducted in Chapter III.

1 The Electric Activity of the Brain

1.1 Neuron Basics (39: 1-5)

The neuron, or nerve cell, is the basic component of the brain which allows for the generation of electric potentials in the brain. Neurons are generally separated by glial cells which basically provide the structural and metabolic support for the neurons. The human brain is believed to be composed of 10^{11} neurons, of a variety

of different classes, and generally share three common features: the cell body (soma), the dendrites, and the axon. Dendrites branch repeatedly from the soma and basically act as the surface on which the neuron receives incoming signals. The axons, which are generally longer than the dendrites, differ from dendrites in their outer membrane properties as well. The axon tends to extend away from the soma and branches near its end, where communication with other neurons takes place. This communication takes place at specific points of contact called synapses. A single neuron may contain one to ten thousand synapses and may communicate with a thousand other neurons. The propagation of an electrical impulse through an axon to a synapse is the result of the special properties of the cell membrane.

The cell membrane consists of two layers of lipid (water insoluble fat) molecules. Differences in cell membranes are due to the various proteins which may be either embedded in the lipid layers (intrinsic) or simply extend from the membrane surface (peripheral). These proteins can be divided into five classes: pumps, channels, receptors, enzymes, and structural proteins. As classes, these proteins are not mutually exclusive. In other words, a particular protein may belong to more than one class. The different behaviors of these proteins allow for the generation of varying electrical signals.

1.2 The Resting, Action, and Postsynaptic Potentials

Electrolytic solutions can be found both inside and outside of the neuron. These solutions include varying concentrations of sodium (Na^+), potassium (K^+), calcium (Ca^{++}), Magnesium (Mg^{++}), Chlorine (Cl^-), and Phosphate (PO_4^{3-}) ions. Na^+ concentrations are roughly 10 times greater outside the cell and K^+ concentrations are roughly 10 times greater within the cell (39: 5). Based on the cell type, this disparity in Na^+ and K^+ concentrations, in addition to the other ion concentrations,

will produce resting potentials ranging from -50 to -100 millivolt (mV) with respect to the outside of the cell, when calculated using the Nernst equation (25: 52,53; 39: 7; 43: 1; 53: 7). Both the Na^+ and K^+ are capable of migrating through the cell membrane. The cell membrane is generally more permeable to K^+ than to Na^+ at the resting potential. However, the permeability of the cell membrane to Na^+ may increase due to electrical or chemical stimulation to the membrane or through an actual mechanical damage to the membrane (25: 56). An increased flow of Na^+ can then cause the resting potential to fall below a critical level, at which point an action potential is generated. The action potential spreads along the axon until it reaches the synapse where a neurotransmitter substance is released. This neurotransmitter then interacts with a receptor on the membrane of another neuron, where it may create an inhibitory postsynaptic potential (IPSP) or an excitatory postsynaptic potential (EPSP) (53: 10). An EPSP will generally increase the permeability of the cell membrane to Na^+ and, therefore, increase the likelihood of the creation of more action potentials or firing. In comparison, an IPSP will increase the permeability to potassium or chloride ions and thereby decrease the likelihood of generating an action potential.

Action potentials are, in themselves, too short (1 msec) and too localized to propagate across cells to be recorded by an electrode located on the scalp (53: 11). However, the temporal summation of the postsynaptic potentials of the synapses of groups of neurons generates a potential large enough to allow a scalp electrode of an EEG to record a 10 - 100 microvolt (μV) signal (53: 11). Therefore, it is the inhibition and excitation of the neurons cell membrane, in addition to the ion fluxes through the cell membrane, which allows for the generation of postsynaptic potentials which can be recorded by an EEG. One would tend to believe the nature of the generation of these signals would indicate a randomness in recorded signals.

For reasons still unknown, a definable rhythm does exist but is believed to be due to the brain's thalamus functioning in a way comparable to a pacemaker (53: 13-15).

2 The Vestibular System

2.1 Basic Function

Having considered how the brain generates electric potentials on a small scale, a brief description of the principal structure believed responsible for influencing the brain's electrical signals during motion sickness follows. This structure, the vestibular system, basically comprises the nonacoustic portion of each inner ear. The main function of the vestibular system is to provide senses of balance, stability, and orientation. The vestibular system also acts in coordinating eye movements. For example, if one spins in circles and suddenly stops, a reflex motion of the eyes results in the perception of the world spinning around them until the vestibular system provides an accurate orientation to the eyes to control this movement. The over-stimulation of the vestibular system through motion or physical damage may result in vertigo, ataxia (muscular incoordination), nausea, and vomiting (49: 85-6). Two principle components of the vestibular system are primarily responsible for its function, the semicircular canals and the otilith organs.

2.2 The Semicircular Canals

Three semicircular canals respond to angular or cross-coupled (Coriolis) angular accelerations (47: 536). The three canals are arranged orthogonally (at right angles) to each other and, therefore, can represent a three-dimensional space. The canals are oriented approximately 45 degrees from the frontal and sagittal planes. Each of the canals is filled with a viscous fluid called endolymph and, upon rotation of the head, the inertia of the fluid causes the fluid to remain stationary. However, there will be a relative flow of endolymph opposite in direction to the rotation of the head.

This relative flow of endolymph will cause sensory receptors (hair cells) located within an area at the end of each canal (the ampulla) to generate a signal which travels down the vestibular nerve to provide information on the rate and direction of rotation of the head (25: 612). The rates at which these signal discharges occur has been shown, in animals, generally to increase with increasing rotation (25: 613). A lateral view of the semicircular canals can be seen in Figure 1.

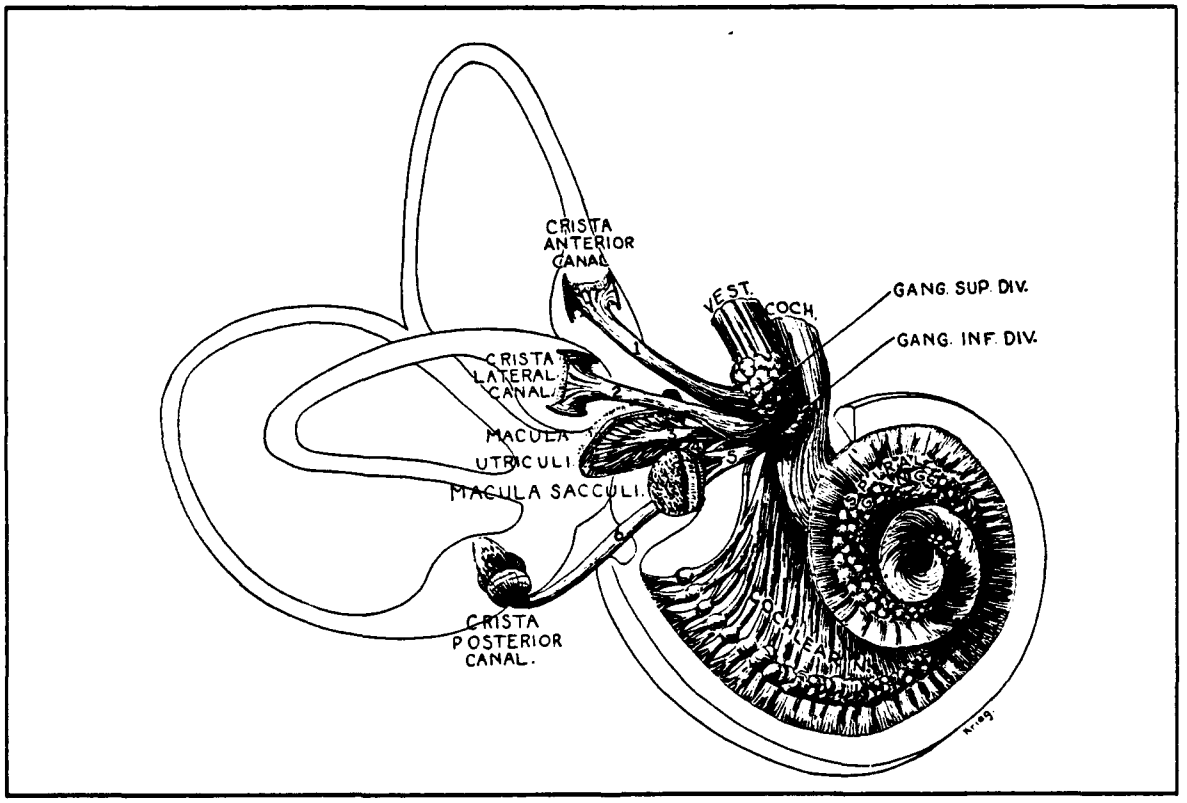

Figure 1. The Vestibular Apparatus. A lateral view of the vestibular apparatus of the left ear is shown with a cut-away view of the otilith organs (Reprinted 38: 143).

2.3 The Otilith Organs

The otilith organs located in a sensory area (macula) within the utricle and saccule of the vestibular system are responsible for determining linear and gravitational accelerations, and static forces (47: 536; 25: 613). The macula of the utricle and saccule lie horizontally and vertically, respectively, and provide a role in determining the orientation of the head with respect to gravity or acceleration. These features are

designated in Figure 1. Each macula is covered by a gelatinous substance in which small calcium carbonate crystals (otiliths) are suspended. Similar to the the semicircular canals, sensory receptors which detect movement of the otiliths relative to the otilith membrane generate signals. Figure 2 provides a enlarged view of the otiliths and its nerve connections. As the force upon the otiliths changes with gravity or head movement, the sensory receptors transmit appropriate signals to the brain which will work to establish an equilibrium (25: 611).

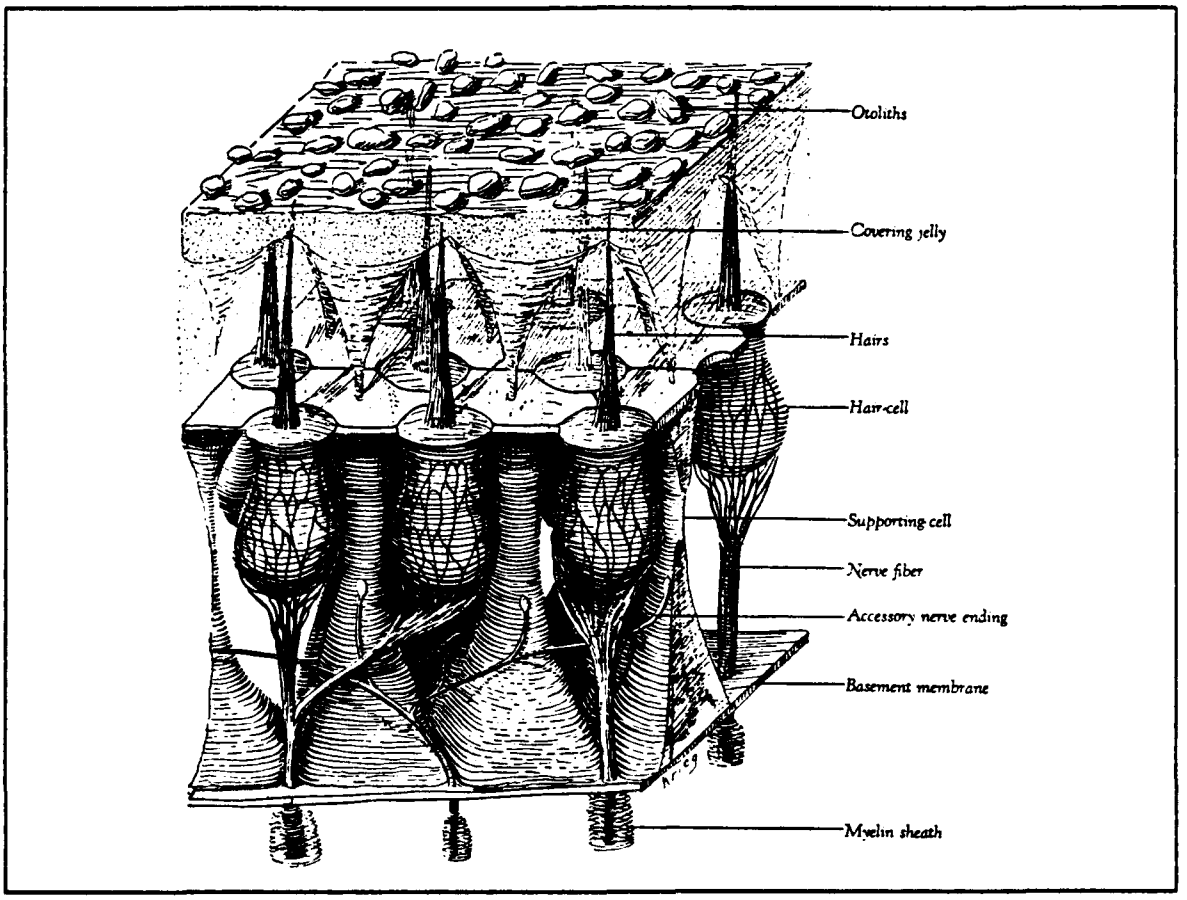

Figure 2. The Otiliths. A cut-away view of the macula and associated endings of the vestibular nerve (Reprinted 38: 146).

2.4 The Motion Sickness Connection

How does the vestibular system relate to motion sickness? First, the vestibular system is part of a very complex series of central nervous system (CNS) connections.

Signals from the semicircular canals and otiliths organs are known to propagate along first-order neurons to the vestibular nuclear complex within the brain stem (Figure 3), the cerebellum, and the reticular formation (47: 546). These connections, in addition to the many second-order connections, are shown schematically in Figure 4. The interrelationship between the signals transmitted by the canals, the otiliths, the visual system, and other sensory receptors is believed to be responsible for the development of motion sickness in what is normally known as the Neural Mismatch or Sensory Conflict Theory (12: 474+; 49: 86+).

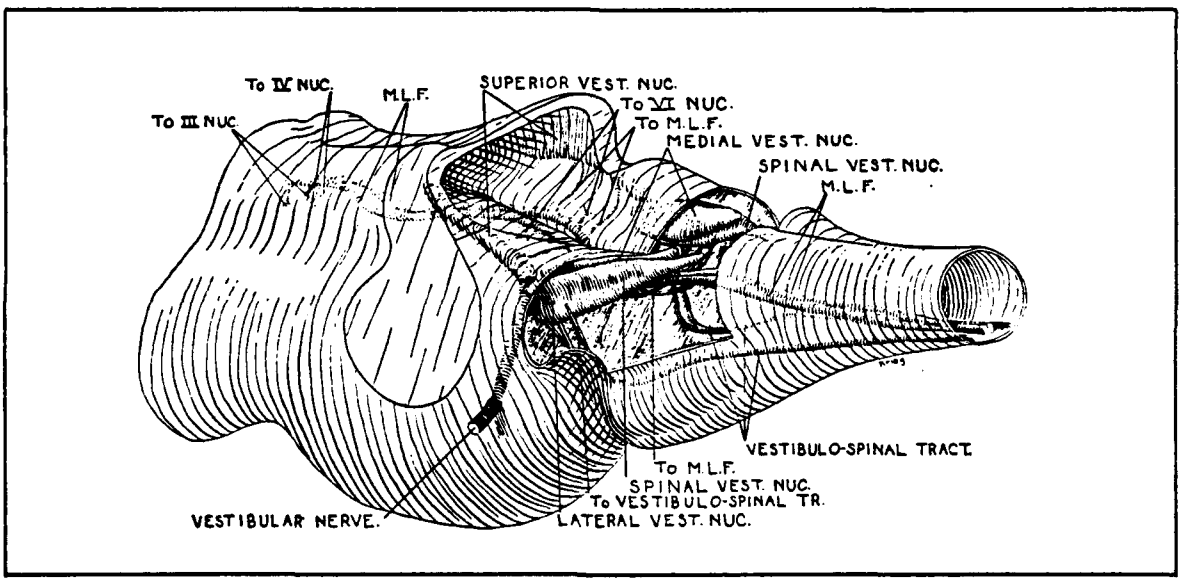

Figure 3. The Vestibular Nucleus. Cut away view of the brain stem revealing vestibular nuclear complex (Reprinted 38: 148).

In short, the Sensory Conflict Theory follows the idea that signals transmitted by the vestibular, visual, and other sensory systems are inconsistent with the signals the individual has learned or expected to receive. The result is the generation of what could be considered an error signal. Depending on the intensity or degree of error, this signal functions to adjust or adapt to the unusual signals. Generally, it is the strongly mismatched signals that create the nausea and vomiting common to motion sickness, which, perhaps, should more properly be called an adaptation syndrome.

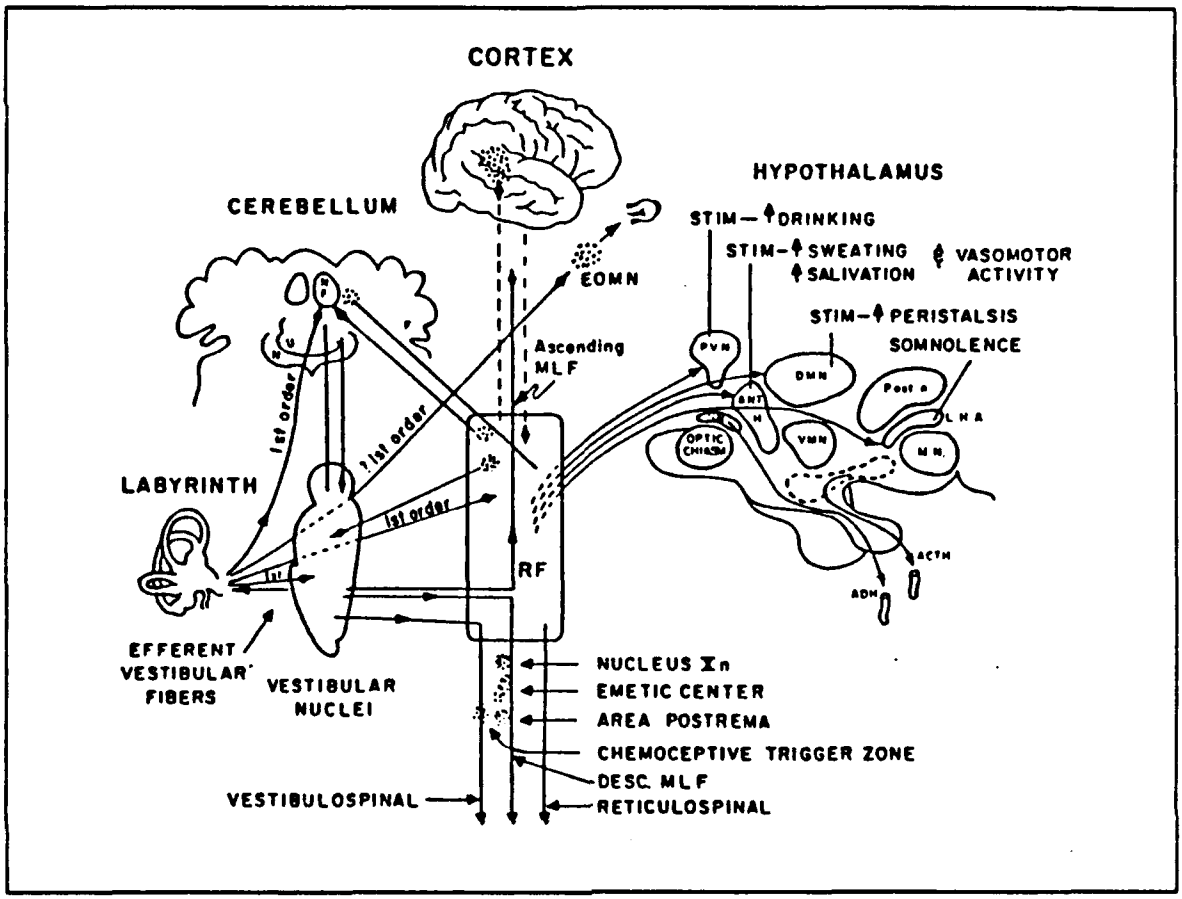

Figure 4. CNS Vestibular Connections. The possibly abnormal activity is depicted with dotted lines. NF = fastigial nucleus; U = uvula; N = nodulus; F = flacculus; EOMN = extraocular motor nuclei; MLF = medial longitudinal fasciculus; RF = reticular formation; PVN = paraventricular nucleus; SN = supraoptic nucleus; Ant. H. = anterior hypothalamic area; DMN = dorsomedial hypothalamic nucleus; VMN = ventromedial hypothalamic nucleus; Post. N. = posterior nucleus; LHA = lateral hypothalamic area; MN = medial nucleus (Reprinted 47: 546).

Two main types of sensory conflict have been described by Dhenin. These types include the visual/vestibular mismatch and the canal/otilith mismatch. Two types of conflict can occur in either of these cases. Either both systems can concurrently signal contradicting information, or signals from one system may be present in the absence of a signal from the other (12: 477). Exactly why these conflicts result in emesis remains unknown.

3 The EEG and EEG Analysis

Having provided a basic background in the generation of electric signals in the brain and the capability of the vestibular system to transmit unexpected signals, the role of the electroencephalogram (EEG) in understanding these signals can now be discussed. A consideration of the basic components and characteristics of the EEG and a look at some of the considerations, problems, and techniques of EEG analysis now follows.

3.1 The EEG

The electroencephalogram, a written record of the electrical activity in the brain, has been a useful tool for diagnosing injuries and brain disturbances, and for studying functional states of the brain since Berger published the first EEG in 1929 (29: 451; 57: 2). EEG data has been collected with anywhere from 8-124 electrodes positioned on or in the scalp. These electrodes record changing brain potentials with time. Electrode placement was standardized by the American EEG Society in 1980 with the International 10-20 System based on use of 21 electrodes (Figure 5). However, depending on the number of electrodes available and the application, variations of the 10-20 system are common.

The frequency content of a recorded signal has proved important in making an assessment of an EEG since its inception. The basic notation introduced by Berger is still used. This notation breaks the EEG into four main frequency ranges: delta (below 3 Hz), theta (3-8 Hz), alpha (8-13 Hz), and beta (13 Hz and greater) (25: 711; 29: 451). Each of these ranges are generally characteristic of certain types of brain activity.

The EEG of a normal adult is generally dominated by rythmic alpha activity during periods of relaxed wakefulness (25: 711; 28: 57; 29: 451). Alpha activity,

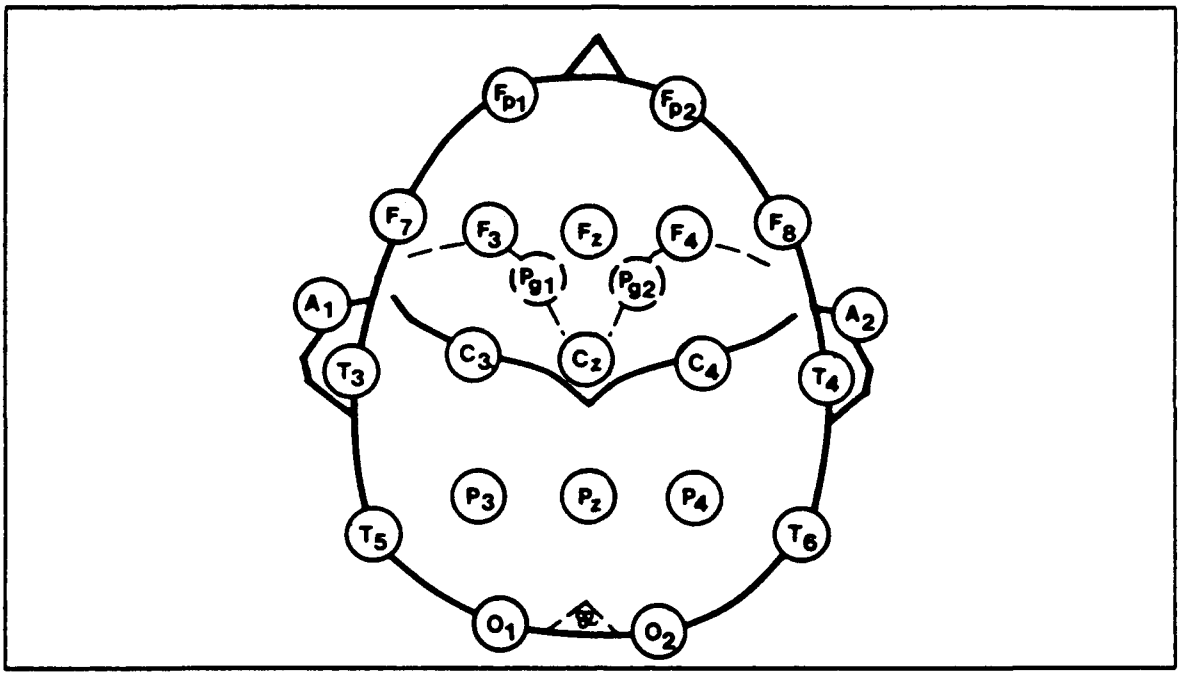

Figure 5. International 10-20 System. Placement and letter-number designation are shown (Reprinted 43: 42).

generally, is clearly seen in the posterior half of the head over the occipital, parietal, and posterior temporal regions and appears to be of greater amplitude over the dominant hemisphere, although the issue of handedness is inconclusive (43: 73). Alpha activity has been shown to have a mean of 10.2 $\pm$ 0.9 Hz and shows a constant waxing and waning (25: 712; 43: 72,73). Alpha activity is highly dependent on an individual's state of vigilance, tending to fall to the theta range with signs of drowsiness, or attenuated with increased mental activity (25: 711; 29: 451; 43: 74). Generation of alpha activity in the cortex is believed to be caused by the thalamic portion of the reticular activating system (25: 712).

Beta activity is seen mostly during increased mental activity or during an intense activation of the central nervous system and rarely exceeds 30 microvolts (25: 711; 43: 80). Theta activity, presumed to be of thalamic origin, prevails mainly in children and reduces with maturation (over 25-30)(43: 83). Theta activity will also manifest itself in adults during periods of disappointment, frustration, or anxiety (25: 712).

This fact may prove useful in interpreting theta activity of motion sickness influenced EEGs due to the correlation Fox and Arnon have shown between levels of anxiety and the progression of motion sickness symptoms (17).

Delta waves can often be seen in periods of deep sleep but are also readily seen when the brain is suffering from injury, disease, or severe trauma, and even in epilepsy and motion sickness (6: 1024; 25: 712; 29: 452; 30: 1255). The relationship of delta activity to abnormal electrical activity in the brain makes the delta band extremely important in searching for a pattern of propagation in the development of motion sickness.

Knowledge of the characteristics of the above frequency bands allows an EEG analysis to proceed by generally looking for deviations from the normal. Before conducting an EEG analysis, however, the capabilities and limitations of the EEG must be understood.

3.2 Problems and Considerations

Prior to conducting any EEG analysis, the EEG record must be looked at for appearances of artifacts. Artifacts are defined as "any disturbance in the recording which does not arise from the brain" (28: 45). Artifacts can have many causes: muscle, electrode, or eye movement; electrode pop; sweating; vascular activity; swallowing; and noise produced by spectral processing (28: 45-52; 46: 170). Artifact may also be introduced during computer processing by smearing the data during filtering or sampling (46: 170). If artifact data is not excluded, an EEG analysis may provide misleading or meaningless results (15: 493; 46: 170).

Another factor to be considered is that data sampling needs to occur at twice the rate of the highest frequency in the signal: the Nyquist Criterion (35: 629; 41: 536). Sampling at less than this rate can result in aliasing, which causes a higher frequency to be represented as a lower one (35: 629; 41: 536). The possibility of this problem

can often be eliminated through use of sharply attenuated high-frequency filters. Such devices will not allow frequencies beyond a certain range to be collected.

The final major consideration to be made concerns the number and placement of electrodes to be used in data collection. In short, spatial resolution increases with the number of electrodes, but large numbers of electrodes may become impractical due to expense and subject discomfort and preparation time (35: 632; 41: 537). Differences in the size and shape of an individuals head will result in variations of electrode placements despite use of a standardized placement system. Finally, it should be remembered that the purpose for the EEG analysis should determine where electrodes are to be placed.

4 Motion Sickness, A Partial Seizure?

As mentioned in Chapter I, the appearance of high-amplitude delta waves, during the development of motion sickness, indicated a possible link of motion sickness to epileptic events or partial seizures. Is there a connection to an epileptic event? Can an understanding of seizure development provide clues to finding a pattern in the development of motion sickness? These answers are not clear, but a knowledge of the common characteristics of a partial seizure and the common features of an EEG-recorded seizure may prove useful.

4.1 The Partial Seizure

Partial seizures are one of two general classes of seizures defined by the 1981 International Classification of Epileptic Seizures. In general, partial seizures are those in which "the first clinical and EEG changes indicate initial activation of a system of neurones limited to part of one cerebral hemisphere" (13: 11). Partial seizures have been classified according to whether consciousness becomes impaired. During a complex partial seizure, consciousness is impaired, but in a simple partial

seizure, it is not. The term impaired consciousness refers to "the inability to respond normally to exogenous stimuli by virtue of altered awareness and/or responsiveness" (13: 11). The lack of impaired consciousness in motion sickness will narrow any comparisons to the simple partial seizure.

The following signs or symptoms are common in the occurrence of simple partial seizures: motor signs, somatosensory or special sensory symptoms (visual, auditory, olfactory, gustatory, vertiginous), autonomic symptoms, and psychic symptoms (much more common in complex seizures) (13: 11). Motion sickness bares closest resemblance to a simple partial seizure with autonomic signs. Epigastric sensation, pallor, and sweating are common symptoms to each.

Unfortunately, without consciousness being impaired, simple partial seizures have often been neglected and have gone unrecognized due to difficulty in distinguishing between simple seizures and nonepileptic disorders (which motion sickness may or may not be) (11: 1347, 1350). The diagnosis of a simple partial seizure, however, often occurs after an EEG reveals seizure-like discharges. Limited studies of EEGs recorded during simple partial seizures have not always shown abnormalities, but for cases where abnormalities are present, the EEG has often shown single hemispheric involvement and occasional bilateral involvement (11: 1351; 13: 11). The fine lines in classifying some nonepileptic disorders and simple partial seizures leaves the case of classifying motion sickness open for further research. The presence of abnormal EEG during motion sickness, nonetheless, warrants a brief discussion of some basic characteristics of seizure development.

4.2 Seizure Characteristics

John Hughlings Jackson's claim that the signal symptom of a partial seizure is localized to a specific area of the brain has been the foundation of partial seizure

studies since 1866 (11: 1347; 13: 9; 43: 339). Gale has also stated: "seizure activity does not spread randomly throughout the brain but is generated and propagated by specific anatomical routes" (18: S15). Seizure activity is generally characterized on EEG records by the presence of spikes or spike wave complexes in a range of frequencies. The following guidelines exist for the presence of a seizure-like (ictal) event and for an epilepsy. For an ictal event there is:

(a) a sudden change in frequency which appears slowly and then more distinctly to dominate an EEG record;

(b) a sudden increase or loss of voltage (43: 156).

For an epileptic event there must be a focus which will spread its activity and manifest itself clinically (28: 125). Once a focus has developed it may develop into two or more foci either on the opposite hemisphere (mirror focus phenomena) or on the same side due to a constant firing of an original focus ipsilaterally (28: 126). Although briefly stated, these characteristics should be sufficient to aid in the interpretation of an EEG analysis.

5 The Phenytoin Influence

Possibly important to the EEG analysis in this study is the effect the anticonvulsant drug, phenytoin (Dilantin), may have on the EEG. Phenytoin, the most thoroughly studied anticonvulsant agent, was first developed by Biltz in 1908, and shown to have anticonvulsant effects by Merritt and Putnam in 1938 (48: 452). Physiological and psychological measures have shown no consistently attributable effects to Dilantin under normal clinical dosing (4). Blood levels between 10 and 20 µg/ml generally are in the therapeutic range. Toxic levels causing nystagmus, ataxia, and lethargy normally present themselves at blood levels greater than 20 µg/ml.

Phenytoin is believed to inhibit the loss of Na^+ from nerve fibers, thereby reducing excitability and inhibiting the spread of impulses without causing CNS

depression (23: 682; 48: 452). The capability of phenytoin to limit the spread of seizure activity from its focus is greater than its effect on influencing the stimulation threshold (48: 452). The inhibitory nature of phenytoin may influence the EEG. Increased delta activity is normally seen under toxic phenytoin levels and may be present under normal levels (43: 485). Therefore, any effect of phenytoin on the EEG will most likely be detected in the delta frequency band.

An understanding of the effects phenytoin may have on the EEG, in addition to the complex role the central nervous system plays in the development motion sickness, and the basic characteristics of the normal EEG and the partial seizure, provide sufficient background for proceeding with this study. Keeping this information in mind, a derivative of standard analog EEG analysis, brain topographic mapping, will now be considered. Chapter 3 will take a look at the some of the considerations in and methods of brain mapping.

III Brain Topographic Mapping

The search for a motion sickness propagation pattern through an EEG analysis, in the most complicated sense, is an attempt to locate the source of electrical activity within a volume (the brain), given a set of electric potentials from the surface of that volume (43: 704). Use of only scalp electrodes makes the search for an exact location very difficult, but sufficient enough to provide a general idea or indication of a possible location. Since raw EEG data may contain not too little but too much information, the analysis of raw EEG for such patterns may prove arduous (14: 445; 40: 173; 56: 281).

With interpretation of EEG being an art as much as a science, the growth of brain topography as an analytical tool is proving to be valuable. In 1947, in an attempt to create a visual image of the standard analog EEG, Walter and Shipton demonstrated the ability to *visually project an EEG onto a spatial* coordinate system (56: 282). Their device, the first toposcope, used a large cathode ray tube to display modulated light beams controlled by the output of 12 amplifiers, and represented the advent of EEG analysis by topographic (brain) mapping. With advances in digital computing and color video technology in the 1970s and 1980s, the practical use of brain mapping has been on the rise.

Chapter III will present the basics of the topographic mapping technology focusing on its capabilities and limitations. Methods of finding usable features in topographic mapping, specifically, amplitude peaks, spectral analysis, or some type of statistical measure, will also be considered.

1 The Brain Mapping Environment

The capability of brain mapping to describe the location of a raw EEG feature in a way understandable to the inexperienced EEG reader has contributed to the

growing use of the brain map as a communication or teaching tool (46: 166). However, the pretty pictures, depicting EEG spatial properties produced through topographic mapping, can easily be misinterpreted if the methods used are not understood.

A major point of consideration is that a brain map is merely an interpolation of a limited number of real data points (the electrodes) through a mathematical, not physiological, process (35: 632; 46: 169). This is unlike images produced by Computerized Axial Tomography (CAT) or Magnetic Resonance Imaging (MRI), where the majority of points displayed are real. As a result, the attainable spatial resolution, related to the spatial aliasing error, becomes limited by the number of electrodes, which are limited due to practical purposes (41: 537; 43: 705). A result of this limitation was the development of a variation on the International 10-20 System (Chapter II) by Chatrian. Chatrian's 10 percent System places electrodes halfway between each of the International 10-20 locations to provide for adequate spatial resolution through use of a variety of interpolation schemes (41: 537).

A classical method of interpolation has been through the 4 nearest neighbor approach where imaginary data points are computed based on the values of their 4 nearest neighbors (20: 373). Similarly, Duffy has used a 3 nearest neighbor approach in the brain electrical activity mapping device (BEAM) he developed in 1979 (14: 456). Unfortunately, these approaches suffer from the location of extrema at electrode sites, as well as fairly rough interpolated surfaces. Several other methods have been developed to solve these problems. In 1987 Perrin developed a two-dimensional spline interpolation algorithm which allowed for smoother surfaces and more precise estimations (20: 373). Lopes da Silva suggested the use of a Laplacian operator to reduce spatial blurring distortions at the scalp (41: 537). The Laplacian operator, the divergence of a gradient vector, converts the potential measured at an

electrode to a value representing the current density entering or leaving that point (41: 538). Use of the Laplacian operator is similar to use of the two-dimensional spline interpolation in that the derivative of the spline function provides the current density (20: 373). Despite the capability of an interpolation scheme to produce quality maps, a relative degree of distortion should be expected at the brain map edges due to the effects of calculating points near the edge electrodes (35: 632).

2 Brain Mapping Considerations

Before proceeding to specific methods of topographic analysis, some general considerations will be given. The first, and probably most important, idea supported by the literature is that the physiological value of a brain map is increased through proper support by raw EEG data (14: 455; 35; 41: 549; 44; 45: 125; 46). Second, the use of adjustable color scales in topographic mapping provides the possibility of obtaining misleading results due to the capability to overemphasize insignificant results or to underemphasize significant results (35: 632; 41: 539). The capability to obtain lateral and superior views of the brain also has its own advantages and disadvantages. A lateral view provides a clear view of the temporal lobe but requires a map of both the left and right sides to assess symmetry. A superior view, however, may distort information from the temporal lobe but offer a look at both hemispheres. The final consideration, previously discussed in Chapter II, is the importance of removing or limiting artifact.

Once aware of the key considerations of brain mapping, decisions must be made regarding which electrode reference scheme to use, how much data to analyze, and what method to use. The electrode reference scheme, as mentioned in Chapter II, will depend on the purpose of the study. Different schemes (e.g., monopolar, bipolar, linked ears) will affect the appearance of the brain maps (41: 537). An

obvious conclusion is that a standardized reference scheme is important. Next, the proper amount of data to sample is open for debate but is dependent on the purpose of the study. Whether the objective is to look at a steady state condition or a spatially dynamic one, the fact that EEG features are not stationary but wax and wane over time must be considered when trying to determine a proper sample size (35: 629; 46: 170). Finally, the goal of the study may again influence the method of analysis used. Brief discussions of peak amplitude, spectral, and statistical analysis follow.

3 Amplitude-Peak Approach

Perhaps the simplest way of performing a topographic analysis is to focus on the peak voltages or amplitudes of the spike or delta wave complexes seen in the raw EEG record. This approach has been valuable when clear seizure-like spikes or discharges are present, and when a desire to establish the latency of an evoked potential (stimulus/response activity) is required (8; 20: 372; 22: 705; 36: 544). Spike averaging represents a refinement to this approach. In spike averaging, data from a number of discharges are averaged to effectively reduce background activity and better define the spike or wave complex. The typical approach is to sample a small period before and after the peak of a reference electrode, average several of these samples, and topographically display the results over the sample period. Gregory and Kanazawa used this approach to successfully localize seizure activity in benign Rolandic epilepsy in children (BREC) and in a variety of complex partial seizures (22, 36).

Application of these approaches appears to be feasible, but raw EEG of motion sickness may be too long or too dynamic to efficiently obtain meaningful results. The increasingly apparent delta waves which develop during the evolution of motion

sickness gradually appear in more than one channel, making the selection of the appropriate wave complex for analysis over the large record difficult. The amplitude peak approach may prove more valuable in the analysis of motion sickness records after an alternative method is used to provide insight into the problem.

4 Statistical Methods

Use of statistical and correlational methods of brain topography represent a growing area in this field as the following references suggest (14, 15, 19, 20, 24, 31, 33, 35, 40, 41, 42, 46). The basic idea is to transform certain EEG features into parameters which can be compared to Gaussian or normal distributions for the statistical case, and to well-defined pathological cases for the correlational case. Both cases may require the use of a representative database which takes age, gender, and possibly handedness into account (41: 540; 46: 171). A number of features (transformations) obtained from the spectral analysis of the EEG have been used. Features based on the absolute power, x, of a given band include: x, $\sqrt{x}$, $\sqrt[3]{x}$, $1/\sqrt{x}$, log(x), and log(x+1). Features based on the relative power (absolute power divided by the total band power), y, include: y, $\arcsin\sqrt{y}$, and log[y/(1-y)]. The problem with the statistical approach becomes determining which of these features can best approximate a normal distribution (19: 119).

Duffy, Gasser,and John have done a great amount of work in determining which transformations most closely approximate a normal distribution (14, 19, 30). John determined that the logarithmic transformation, log[y/(1 - y)], where y is the relative power expressed as a decimal, provides the best approximation to a normal distribution for eyes-closed measurements (30: 1256). Gasser confirmed John's relative power results, but also determined the transformation, log(x), where x is the

absolute power, worked sufficiently well and that the transformation, $\sqrt{x}$, was possibly more suitable for delta band values (19: 119, 120).

Once viable transformations are found, comparisons can generally be made through creating z-transform or student t-statistic maps. Z-transform maps basically depict the number of standard deviations an individual observation lies from the mean of a normalized population. The t-statistic, however, represents the statistically different regions of two sets of observations. These statistical techniques have been integrated into two of the more common statistical mapping systems. The BEAM system, developed by Duffy and Lombroso, applies Significant Probability Mapping (SPM), introduced by Bartel and Subach in 1976, to display either t-statistic or z-transform maps as well as the classical topographic maps (14: 455; 40: 173).

John has perhaps developed a more detailed statistical mapping system known as neurometrics. Based on work by Matousek and Petersen, John was able to develop a substantial database of the means and standard deviations of the delta, theta, alpha, and beta bands from a variety of electrode locations (30: 1256). Using the log[(y/(1 - y)] transform of relative power, y, and age regression equations to account for age, the EEG features are subject to a z-transformation and mapped so the probability of an abnormality can then be assessed by parametric statistics (30: 1256; 31: 162). Neurometrics has proved useful for studies of a variety of brain related disorders (30, 31, 33).

Despite the capability afforded by statistical mapping, it suffers from several problems or questions which may limit its widespread use. First, a normalized database, in many cases, may need to be developed. Second, a debate over what EEG data should be considered normal or abnormal may arise. Finally, since EEG data varies over time, it may lack some of the stationarity that would be preferred

for a good statistical analysis (46: 170). Statistical mapping, however, still appears to offer promise in the analysis of motion sickness EEG.

5 Spectral and Dynamic Analysis

Implicit in accomplishing a statistical topographic analysis was the capability to perform a spectral analysis of EEG data. The fast Fourier transform (FFT), which converts a digitized signal in the time domain to the frequency domain, is commonly used in spectral analysis. Available mapping systems often allow the computation of 2-to-4 second FFTs in which any or all of the 4 spectral bands may be represented. If larger sample times (epoches) are desired, the FFT is normally computed by averaging the FFTs of a series of smaller epoches (46: 170). Nuwer has stated "the distributions of various frequency activity can be communicated by maps in a way difficult to specify as well in words alone" (46: 169).

Amplitude and power (amplitude squared) are the common features used in spectral analysis. Power has the tendency to emphasize very active areas while amplitude tends to correlate better with the inspection of a visual waveform, in addition to offering good mid- and low-range resolution (35: 633; 15: 493). Computation of these spectral features does introduce the possibility of broad-band power artifact as a result of the epoch edges. The sampling rate of the EEG must be at least twice the highest frequency contained in the EEG, and the spectral resolution will be limited to the inverse of the epoch size. This last part implies if the largest FFT which can be processed is 2 seconds the spectral resolution will be 0.5 Hz. A spectral analysis is also sensitive to changes in an individual's state of mind and it becomes important to sample a long enough segment of data to be representative of a particular state (35: 629). Keeping these considerations in mind, it seems reasonable to continue the effort of motion sickness spectral mapping

started by Banducci because it appears more efficient than amplitude-peak analysis for large amounts of EEG data without the need for the extra computational capacity and database necessary in statistical mapping.

Before moving on to the methodology used in this thesis, a brief mention of dynamic EEG topography needs to be made. Dynamic topography adds a temporal value to the spatial representations of brain maps. By displaying a series of spectrally processed EEG epoches or simple digitized EEG potentials, the spatial changes in time have proven useful in EEG analysis. The use of dynamic EEG topography with video has allowed the spread of seizure activity to be recorded and easily shown over time (36: 545; 55: 420).

IV Methodology

The EEG data used in this study was collected from healthy normal humans who volunteered, after informed consent, to participate in cross-coupled Coriolis-induced motion sickness experiments. The procedures and protocol were approved by the Human Use Review Committee at Wright-Patterson Air Force Base. The EEGs of ten military personnel, seven male and three female, were subject to topographic analysis in the course of this thesis. Eight of these personnel participated for the purpose of motion sickness data collection only. The remaining two subjects participated in a double-blind phenytoin experiment and provided a total of four EEG records for analysis. Females were prohibited from participating in phenytoin trials due to possible teratogenic effects. A total of 12 EEG records were, therefore, available for analysis.

1 Collection of EEG Data

1.1 Collection Devices

A 14-channel bipolar montage based on the 10 percent placement system mentioned in Chapter III was used in the collection of all 12 EEG records. This montage provided the most diffuse spread of electrodes for the number of electrodes available. The montage is depicted in Figure 6. A special electrode and amplifier system was designed by Chelen to allow the recording of EEG data throughout the period of motion sickness development (7). The system was designed to be mounted to the back of the head so that data collection would be possible during rotation and head movements.

Chelen's EEG collection system was also designed to allow the recording of activity down to 0.25 Hz (sub-delta) which could aid in the investigation of this motion sickness associated trait. Each of the platinum subdermal electrodes (used to

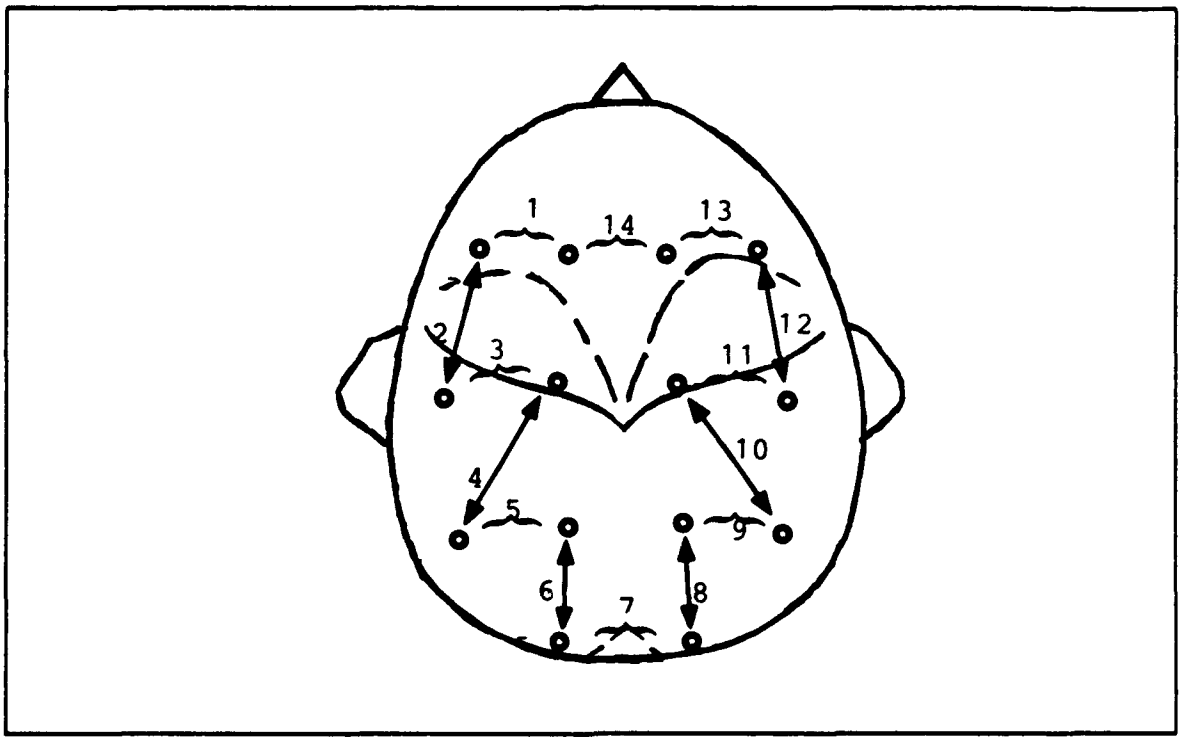

Figure 6. The 14-Channel Bipolar Montage. This montage shows the channels used during the collection of motion sickness EEG data. Signals detected at each electrode are combined to reveal the polarity of the signal in each channel.

prevent the introduction of sweat artifact) were connected to 85 decibel (dB) gain amplifiers. To permit a full-gain capability from 1 to 30 Hz and a 25 percent gain at 0.25 Hz, each amplifier was designed with 3 dB/octave low frequency roll off. The signals from each amplifier were sent through a low-pass filter device and then recorded on tape using a Kyowa-Dengyo RTP-610A data recorder. Each signal was also simultaneously displayed on a Soltec 8K20 strip-chart recorder.

1.2 Collection Procedures

A standardized set of procedures were used in collecting the motion sickness EEG data. Subjects were seated in a Neurokinetics Model 8010 rotary chair where the relatively small electrode amplifier box was strapped to the back of their heads. To minimize any possible eye-blink artifact and visual reference, the eyes were taped

shut and the subject blindfolded. In several cases, additional physiological measurements such as electrocardiograms (EKG), electrosplanchnograms (ESG), and gastrointestinal (GI) stethoscopy, were also taken.

After the subject was seated in the chair, roughly 10 to 15 minutes of baseline data was collected on the subject. During this time, the system was checked to test for any significant contribution of head- or eye-movement artifact. After the collection of baseline data, the chair was rotated at 1 degree/sec^2 about the subject's seated, upright position (z-axis). The chair was accelerated to a fixed speed between 10 and 18 rpm. The rotation speed was selected based on the subject's motion sickness history questionnaire and the results of a susceptibility trial run. The goal was to provide each subject with equally provocative amounts of Coriolis stimulation to illicit an emetic response in similar periods of time. After attaining the fixed rotation speed, the subjects responded to recorded audible commands which directed either left/right/up/down head motions every 10 seconds. Throughout each trial the subjects were queried to report their symptoms and to provide an indication of their subjective sickness level on a scale of 1 (normal) to 10 (imminent emesis). During the collection of EEG data, the strip chart was annotated to indicate all head motions, possible artifacts and potential causes, symptoms and sickness levels, and the Kyowa-Dengyo recorder counter numbers. These annotations would aid in the post-trial analysis. The entirety of each trial was also recorded on VHS tape by chair-mounted and external video cameras.

All but four of the trials used in this analysis culminated in emesis. The other four trials were ended by subject request at levels of frank sickness (severe nausea).

2 Data Analysis

2.1 The A-to-D Conversion

Analysis of the EEG data recorded on tape during each trial was made possible through use of a Bio-Logic Systems Brain Atlas, a PC-based brain topography system. Prior to feeding the EEG data into the Brain Atlas system, several steps were taken to ensure quality results. First, the Brain Atlas was manually calibrated across all channels using a 400 mV peak-to-peak square wave. Next, due to the detection of a slight DC offset produced by a faulty amplifier, a procedure which tested for DC offset using a Tektronix TM 506 oscilloscope was implemented.

The introduction of any DC offset presented the problem of noise or leakage into the lower frequencies of the delta band. The theta, alpha, and beta bands remained unaffected. To eliminate the DC offset, all channels of each record were tested using the oscilloscope. The Kyowa-Dengo recorder had the ability to adjust for any DC offset detected in any channel. In addition to providing a standardized set of data by removing any DC components introduced by the electronics involved, this procedure offered the capability to detect possible electronic component malfunctions which could ruin useful data. After the completion of these two steps, the EEG data was ready for analog-to-digital conversion.

All 14 channels of each EEG record were digitized at 64 samples/sec by the Brain Atlas system and stored either on a hard disk drive or 5.25-inch diskette. The storage capability of each diskette was normally ample enough to save baseline through emesis (or last head motion) EEG data. The digitized data could then be displayed in either raw EEG or topographic form through use of a variety of Brain Atlas functions. The actual interpolation scheme used for determining the brain maps was not available.

2.2 Procedures

Prior to establishing the methods to be used during this analysis, the procedures previously used by Banducci were examined (2). Banducci attempted to look at the FFTs of continuous 2-second epoches. The Brain Atlas has the ability to continuously display 2-second FFTs, revealing up to 12 maps per display. By examining each record using this method, it was possible to conclude certain areas contained an increase in activity but it was difficult to determine the existence of a propagation pattern (2: 124). A general conclusion is that although the 2-second FFT provides an efficient user interface, it is inefficient in establishing the existence of a pattern.

The answer as to how to analyze the motion sickness data stems from an attempt to understand some of the subjective opinions or experiences of the subjects. With the development of motion sickness symptoms and the presentation of sickness levels, it is reasonable to suggest that although the sickness level represents how sick a subject feels, the feelings or symptoms tend to oscillate about a certain level. The fact that certain head motions often prove to be more stimulating than others and the attempts by several subjects to exactly describe the oscillating nature of their symptoms with fractional sickness levels (e.g., 8.5, 8.25) supports this idea. In other words, a waxing and waning nature of a subject's degree of sickness may be related to the waxing and waning nature of the brain's electrical activity. The conclusion is that a 2-second epoch is simply not large enough to represent a subject's overall state or condition. Therefore, the analysis of a large enough epoch to represent a state of time is important.

Based on this philosophy, a heuristic approach was taken in selecting an epoch large enough to possibly represent the state of mind at a specific stage of motion sickness. A period of 10 seconds was chosen primarily because the computational

time required to process individual 10 second FFTs was workable for the amount of EEG data. Another, less important reason, was that a 10-second epoch would allow the inclusion of a portion of head-movement-stimulated activity due to the 10-second intervals between head motions.

Each 10-second epoch was selected using the subjective sickness level reports from each subjects trial as a guide. A Hamming window was employed in processing each 10-second epoch. Baseline and chair acceleration data were also sampled to provide maps to which other, more symptomatic, maps could be compared. Based on the amount of EEG data available for analysis, the epoches were selected at roughly 30-second to 1-minute intervals, or when the subjective sickness level changed during the later stages of motion sickness development. Any portion of a record containing apparent artifact was not included for analysis. However, at sickness levels of 8 or 9, several subjects generated electrical activity which was clipped by the Brain Atlas if it exceeded a certain level. This data was generally excluded unless the maps displayed with or without the clipped data revealed no significant difference.

The FFT of each 10-second epoch was computed through averaging five 2-second FFTs. The 10-second FFTs could not be displayed continuously, but were logged and saved as computer files for later comparisons. Topographic maps representing the square root of power of each FFT were displayed for each of the four spectral bands. The following frequencies were used for each band: delta, .50 - 3.0 Hz; theta, 3.0 - 8.0 Hz; alpha, 8.0 - 13.0 Hz; and beta 13.0 - 23.5 Hz.

To obtain more direct comparisons of the brain maps representing each state, the map analysis function of the Bio-Logic system was utilized. This function allowed direct comparisons of each state by displaying up to 12 maps on the video monitor. Each map represented the amplitude of a single frequency of each FFT. The frequencies presented were chosen based on their proximity to the peak amplitude of

the FFT waveform in the delta band and for its resemblance to the map representing the whole band. The frequencies of 1.0 Hz or 1.5 Hz were normally displayed, although actual FFT peaks appeared to be at less than 1 Hz. Peaks at less than 1 Hz would have required use of a .5 Hz display, a point at which the full-gain of the amplifiers may not have been utilized. The .5 Hz interval (resolution) was due to the capability to only process 2-second FFTs.

After the state maps from each trial were compared, a dynamic EEG was created. Approximately 216 files (maps) created from the baseline through post-emesis record of Subject 5 are continuously displayed as an animation to display the EEG changes during the development of motion sickness. Subject 5 was chosen due to the rapid progression of symptoms demonstrated and due to the almost completely artifact-free record. From baseline data through the first head motion, 6-second FFTs are used, each overlapped by 3 seconds of previous data. For example, an epoch from 30 seconds to 36 seconds followed by an epoch from 33 to 39 seconds and so on. Although one could argue this could blur the changes, this approach allows the gradual changes in power (square root of power) to be seen, since each map contains data included in the previous one. A series of maps with no data in common would show a series of discrete changes which may not provide a clear progression of activity. From the first head motion through two episodes of emesis, 6-second FFTs are displayed at 1.5-second intervals. The remaining data is displayed using 6-second FFTs at 3-second intervals. Three videos were made. One displays maps from all 4 frequency bands, another shows a single map at 1.5 Hz of the delta band, and the third reveals the analog EEG and the corresponding voltage map.

Portions of symptomatic records from several other subjects were also examined to investigate the EEG variations during these periods. These investigations also

used 6-second FFTs but at 0.5-second intervals.

The procedures discussed in this chapter, although not optimal, primarily due to the high degree of user interaction required by the Brain Atlas, were sufficient to provide positive results. Both the state maps and the dynamic EEG revealed the appearance of a propagation pattern. These results are described in greater detail in the next chapter.

V Results

The results of the Coriolis-induced motion sickness trials are displayed in Table 1 for all 12 subjects. The table includes the subject number (Subj), their sex, handedness, chair rotation rate (RPM), the time of the first head motion (1st HM), the approximate time of the last head motion (Last HM) and highest sickness level reported, the time of wretching or emesis (Emesis), as applicable, and the phenytoin blood levels in micrograms per milliliter (µg/ml), if applicable. Handedness was included in the event that trends or differences could be noted in the EEGs of right- and left-handed subjects. The results discussion will first consider the characteristics of baseline maps over all 4 frequency bands. Next, general observations regarding changes noted in these bands during the development of motion sickness will be provided. The focus of the results will then move to the patterns noted in the delta band. The results of the phenytoin trials will also be explained. Finally, the results of the dynamic EEG and associated mappings will be discussed.

1 Baseline Characteristics

The square root of power of each frequency band was displayed using a 16-color scale with a range of 0 to 31.8 µV. The term energy, or power, may be used in describing the brain maps in the descriptions that follow, but the reader is advised it is the square root of power being discussed. An example of a baseline map is shown in Figure 7. All bands from each subject show the expected waxing and waning nature of electrical activity. In all subjects, the delta band is relatively low in power and generally does not exceed 7.9 µV, except in the cases of Subjects 4, 9, and 10 where values near 15.9 µV are seen in the left fronto-temporal, the left parietal-temporal, and the right temporal regions. These locations tend to show higher activity in the other subjects as well, but the differences are very slight.

Table 1. Experiment Results

SUBJ	SEX	HAND	RPM	1st HM MM:SS	Last HM MM:SS	EMESIS MM:SS	µg/ml
1	M	R	12	2:44	26:02 (6)	26:02[1]	0
2[2]	M	R	12	4:05	6:00 (6)	6:37	0
3	M	L	14	3:22	13:52 (6)	N/A	0
4	M	R	16	3:32	8:46 (6)	N/A	0
5	M	R	14	3:10	4:50 (9)	5:17	0
6	F	R	11	2:51	8:47 (8)	N/A	0
7	F	L	16	4:05[3]	5:12 (8)	10:09	0
8	F	L	14	4:37	13:05 (9)	N/A	0
9	M	R	12	5:03	11:29 (10)	11:29	13.8
10*	M	R	12	3:19	6:36 (10)	6:36	0
11	M	R	10	3:18	9:38 (9.5)	9:38	11.6
12**	M	R	10	2:42	11:24 (9.5)	11:24	0

1. Due to the length of this record, data was stored on 3 1.2-Mb disks. The times presented are cumulative totals.
2. Baseline and acceleration data was not used due to failure to operate the low-pass filter on this data.
3. Subject was symptomatic (Level 3). Experiment was restarted due to system malfunction. Nonsymptomatic and acceleration data was available for analysis
* The EEG records of Subjects 9 and 10 are from the same individual.
** The EEG records of Subjects 11 and 12 are from the same individual.

The baseline energy displayed in the theta band was slightly higher than the delta band energy and appeared to be fairly symmetrical. Higher levels were noted in all cases in the left parietal region. The presence of this energy appeared to be primarily attributable to the power contained in the alpha band. The alpha band energy was generally low, except in the left parietal (or posterior) region where it waxed and waned around 31.8 µV. The right temporal area also showed high energy, but less

than that of the left parietal region. The peak alpha frequency of the maps sampled for additional analysis was commonly near 10 - 11 Hz. These results are indicative of the alpha frequency and patterns expected in normal adults during relaxed wakefulness. The theta band of Subject 6, however, appeared to contain more activity than the alpha band in this region, and was possibly due to a lower than normal dominant alpha frequency. The power in the beta band was generally low (7.9 μV) and symmetrical in appearance with the central regions of each map containing the least power. A representative map is shown in Figure 7.

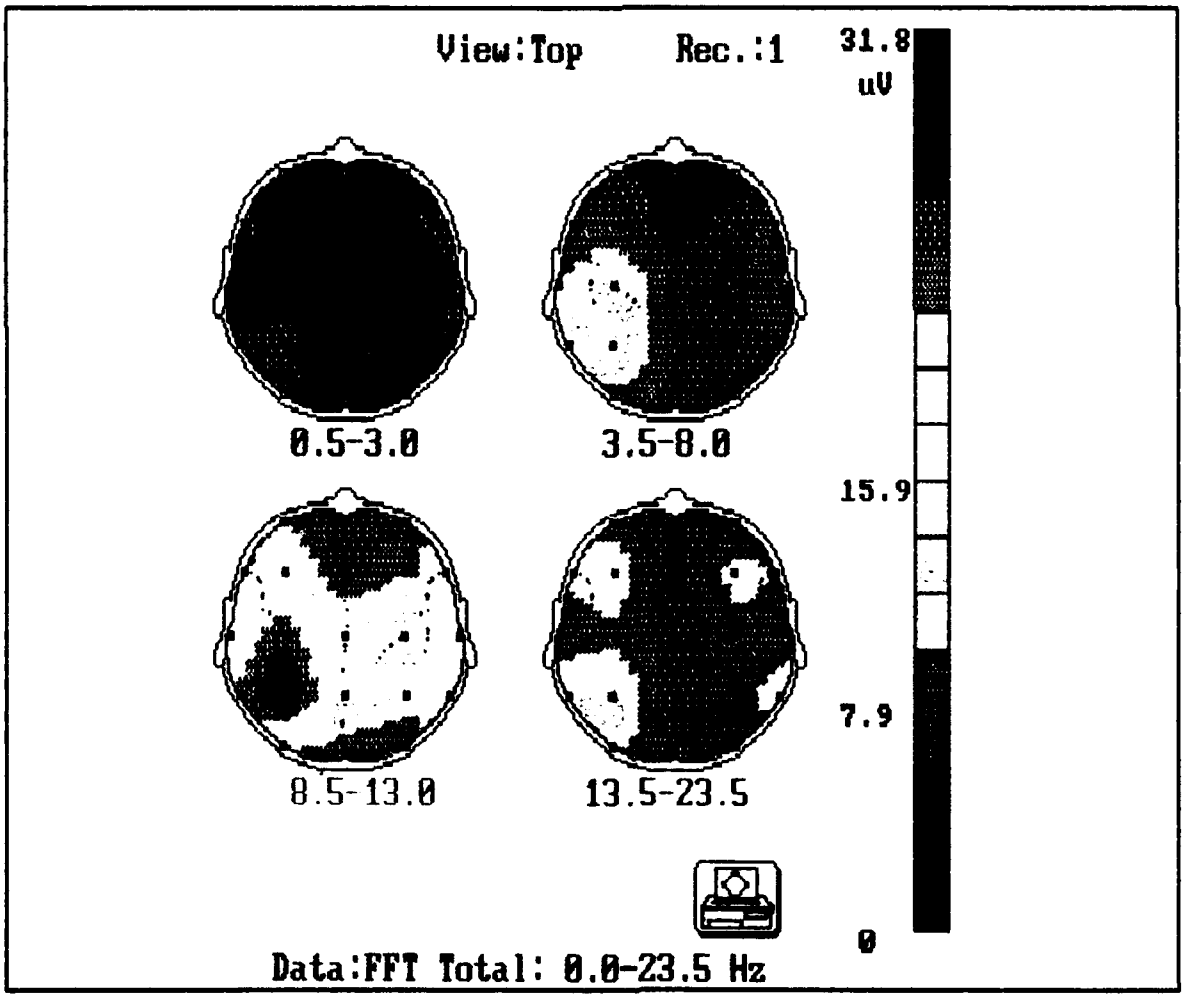

Figure 7. Baseline Maps. The typical energy contained in the four spectral bands of Subject 2 are shown with blue colors signifying less activity and yellow and reddish colors more. Note the dominant activity in the alpha (8.5 - 13.0 Hz) range.

2 General EEG Changes

With the development of motion sickness, no significant changes in EEG activity were observed in the alpha or beta bands. The beta band revealed no changes and all maps appeared very similar to any map which could be generated from a random 10-second sample of baseline EEG. The alpha band power showed a slight overall increase with the development of motion sickness. There were no significant changes in any particular region of each map.

Unlike the alpha and beta bands, significant changes were noted in the delta and theta bands during the progression of motion sickness symptoms. The delta changes are briefly described here and will be discussed in further detail in the next section.

In general, with the earliest signs of motion sickness the delta activity begins to increase in the left hemisphere in the parietal or parieto-occipital area of the brain maps. This increase in power normally is quickly followed by increases in power in the left fronto-temporal region. The power in the fronto-temporal region is typically less than that in the parietal region and its presence, although apparent, is not as constant as the parietal activity. At some point in the progression of symptoms there is a contralateral propagation to the right temporal region. The brain maps also seem to show a slight shift in the parietal activity toward occipital regions when this propagation takes place. The overall power in these localized areas of activity generally increases to exceed the maximum range of the 31.8-μV color scale.

The increases in theta band activity appear to shadow the developments of activity in the delta band. The localized areas of increased theta activity contain less power than similar regions in the delta band. The most visible reason is that the high-amplitude waveforms of the FFTs in the delta region contain significant components in the theta region. By observing the waveforms representing the FFT of each electrode position in Figures 8 and 9, the reader can see how the rolloff from the

delta band remains high into the theta band. The change from delta to theta bands is depicted by the line under each waveform changing from pink to purple. The 21 waveforms correspond with the locations depicted in each map.

Figures 8 and 9 also reveal the characteristics just described at two different symptomatic levels of Subject 9. A more detailed review of delta activity results is now given.

3 Patterns in Delta Development

The determination of the changes in delta activity during the development of motion sickness was the result of repeatedly reviewing the state maps of each subject for trends common to each. An apparent trend did exist. This trend was common to all 12 subjects with a few minor exceptions and can be discussed in three steps. First, a description of the trends as they relate to the increasing severity of symptoms will be provided. Second, peculiarities which were noted will be discussed. Finally, a general pattern which is based on the noted trends will be defined.

The first signs of increased delta activity was generally noted with the initial development of symptoms in all subjects. These symptoms generally included dizziness, queasiness, or cold sweating. The activity was localized to the left parietal area in Subjects 1 - 9 and appeared to be localized a little further back (parieto-occipital region) in Subjects 10 - 12. With the initial appearance of the left parietal activity, a slight increase in activity was noted in the left fronto-temporal region. The maps of Subjects 1 and 3 revealed no change during these early stages. In several cases, data from the period of acceleration revealed slight increases of parietal activity. This could have been caused by slight head movements or a slight imbalance of the rotating chair. These occurrences also may have not been abnormal at all. Subjects 7 and 10 also showed slight increases in activity in the right temporal

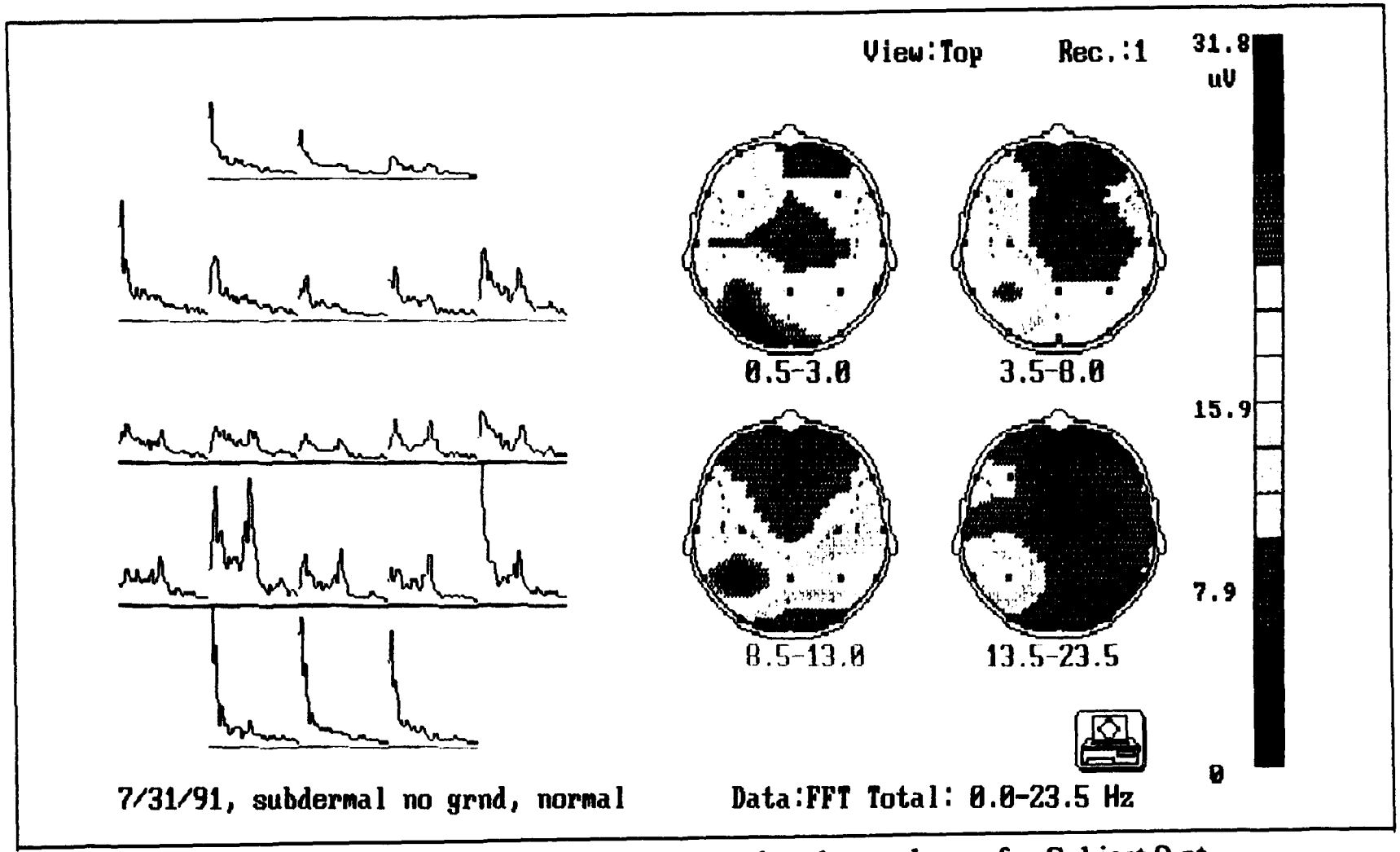

Figure 8. Subject 9 Band Maps. The 4 frequency bands are shown for Subject 9 at Sickness Level 3 (queasiness). Notice how the power as revealed in the delta map and the respective waveforms is close to that typically dominated by alpha frequencies.

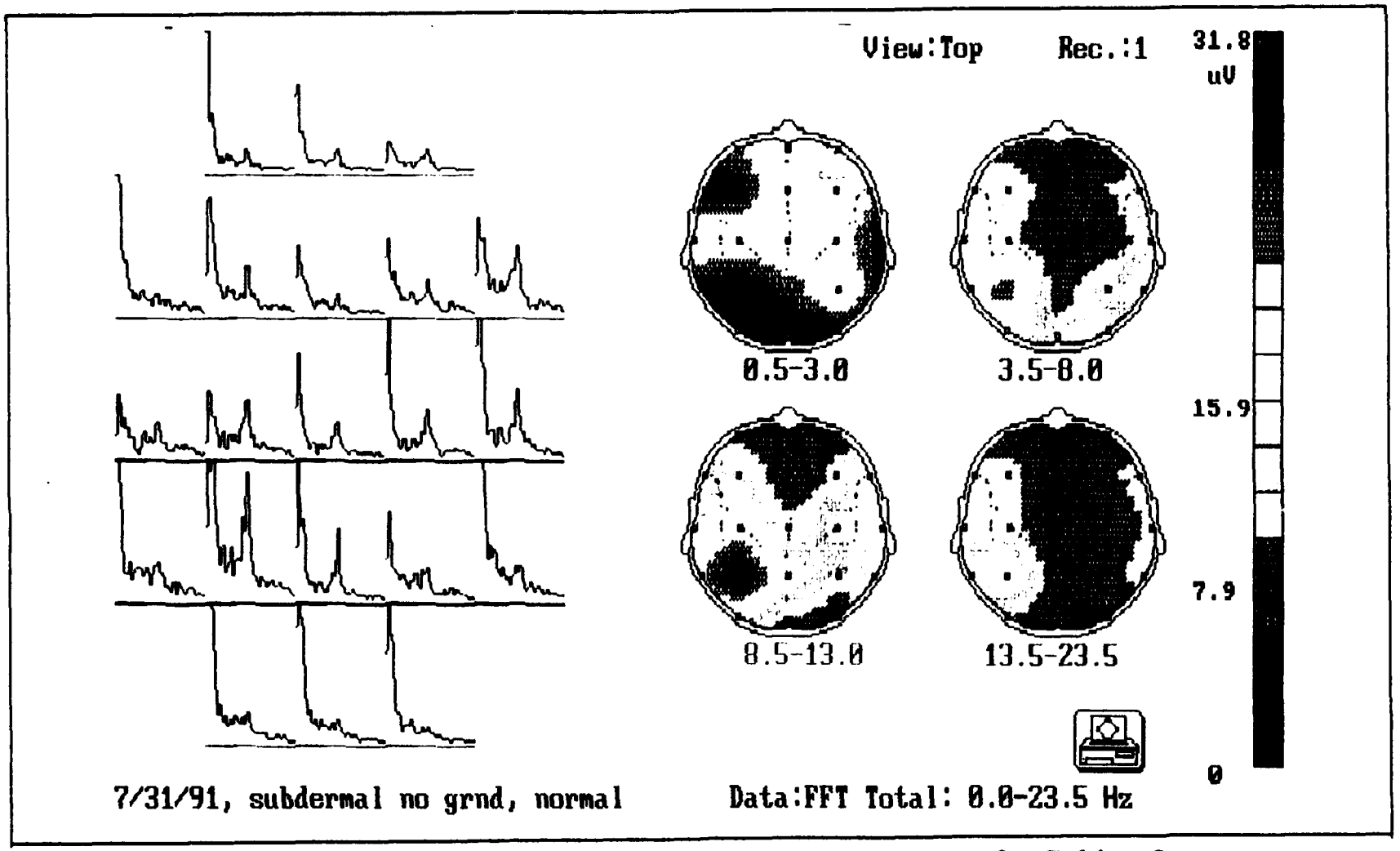

Figure 9. Subject 9 Band Maps. The 4 frequency bands are shown for Subject 9 at Sickness Level 9 (severe nausea). Note the overall growth in delta band power compared to that shown in Figure 8. The right temporal activity is also much clearer at this point.

area at this stage. As the symptoms increased to the first reports of stomach awareness or nausea (generally a 3-to-5 sickness level), the power previously mentioned increased and several additional changes became apparent. Left parietal and fronto-temporal activity was increasingly apparent. The left fronto-temporal activity generally remained less than the parietal activity. Subject 3 still revealed no changes in the left fronto-temporal region. In addition to the increased power displayed in the left hemisphere, the development of right temporal activity was apparent except in Subject 4. The localization was not extremely clear in the majority of the subjects as the activity varied from the anterior to posterior temporal regions. Maps of Subjects 5, 8, and 9 did reveal a clear temporal focus. Another change noted was what appeared to be a spread of the left parietal activity occipitally to the right hemisphere. This does not, however, suggest the electrical activity simply jumped the longitudinal fissure.

With the increasing severity of symptoms toward emesis, an overall increase in power was common to the focal points of activity. Despite the clear build in power overall, there were clear signs of a waxing and waning development. This waxing and waning is revealed by viewing a series of maps in time and noting that a map representing a low sickness level contains more activity than a state map of a higher sickness level (Figure 10). Subject 4, whose trial was ended at Sickness Level 6 (SX 6), nausea, showed no clear sign of localized temporal activity although there was an indication of progression into the right hemisphere. Subjects 5, 8, and 9 maintained a right temporal focus. The remaining subjects showed right temporal activity which, although clearly temporal, was not clearly localized. Figures 10 and 11 depict the changes which occurred in Subjects 1 and 5 using 12 maps representative of the pattern of propagation during motion sickness. The maps are read from left to right. Each map shows the amplitude of a specific frequency of the FFT and,

therefore, compared to the full-frequency band map uses a color scale of shorter range. Maps which contain several samples over one sickness level are signified by the sickness level and a letter (e.g., SX 6A, SX 6B). Some figures also contain post-emesis maps which can be used to compare how accurate a subject is in quantifying their degree of sickness in relation to their brain waves. State maps of the remaining subjects can be found in Appendix A.

Several peculiarities of the analyzed maps did appear and should be noted, although not common enough to be considered trends in the development of motion sickness. The first and most common is that the left frontal activity was not always clearly present in the various samples taken during the evolution of motion sickness. However, the other focal points, despite the waxing and waning, appeared more established once developed. Could the firing in the left parietal lobe be due to the activity in the fronto-temporal region or is it due to something else?

Second, there were several cases of increased activity in both frontal lobes during the more symptomatic stages. The more common occurrences were seen in Subjects 3, 6, and 12. These appearances may be due to increased eye activity during the later stages of motion sickness or they may be due to actual undetected eye-motion artifact. If it is eye artifact, why was it not detected to any clearly significant degree during the prerotation eye calibration?

The final peculiarity was noted to be common to the three left-handed subjects (3, 7, and 8). At moderate to severe symptom levels, the left parietal and fronto-temporal activity occasionally faded into a more temporal focus. The original foci did reestablish, however. This may represent activity in some cortical pathway between the two foci or a relationship to handedness. A determination of the real cause will require a much more detailed analysis and a larger subject pool. Figure 12 depicts the occurrence of this situation for the three left-handed subjects.

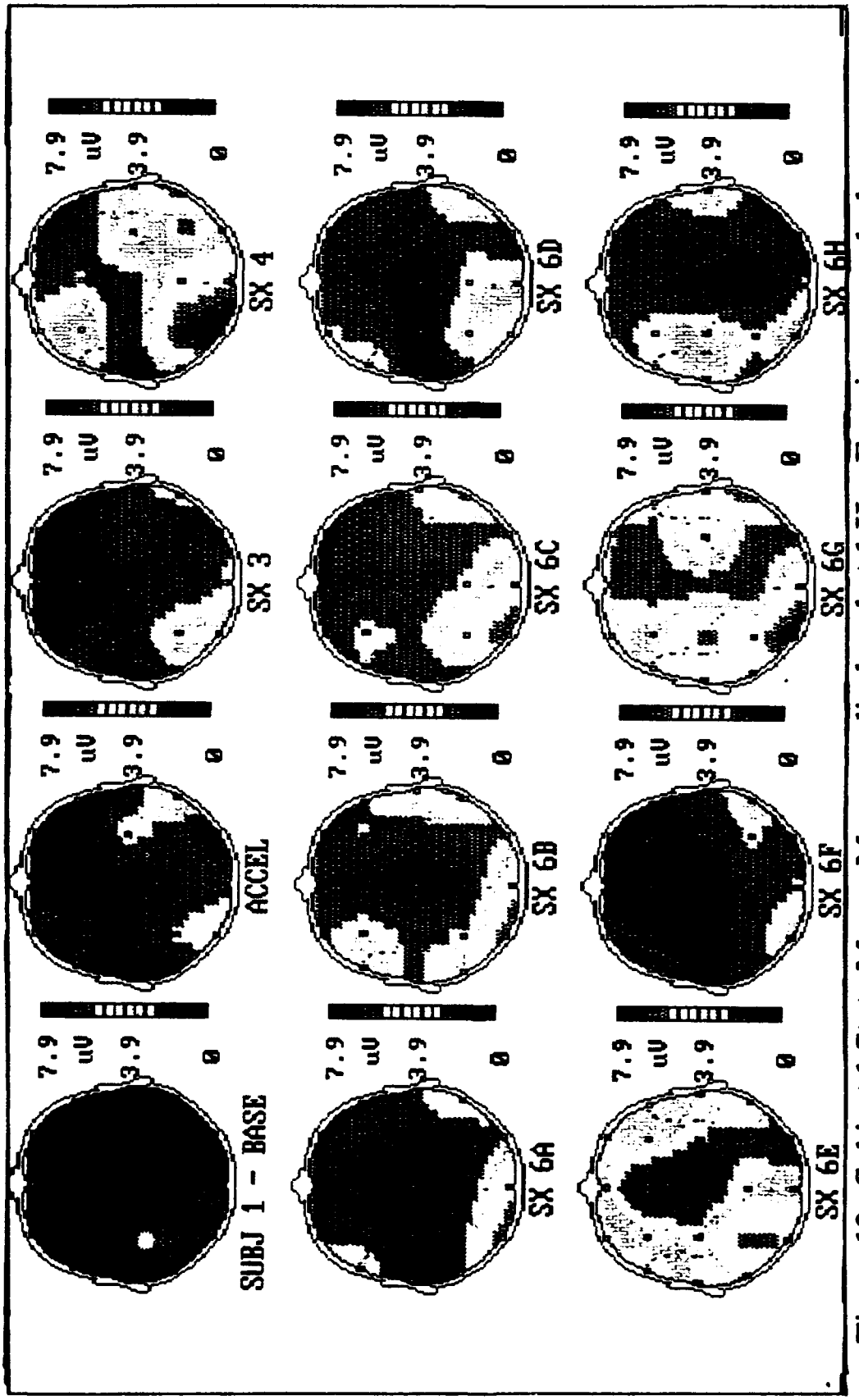

Figure 10. Subject 1 State Maps. Maps are displayed at 1 Hz. Emesis was reached several seconds after the SX 6H map.

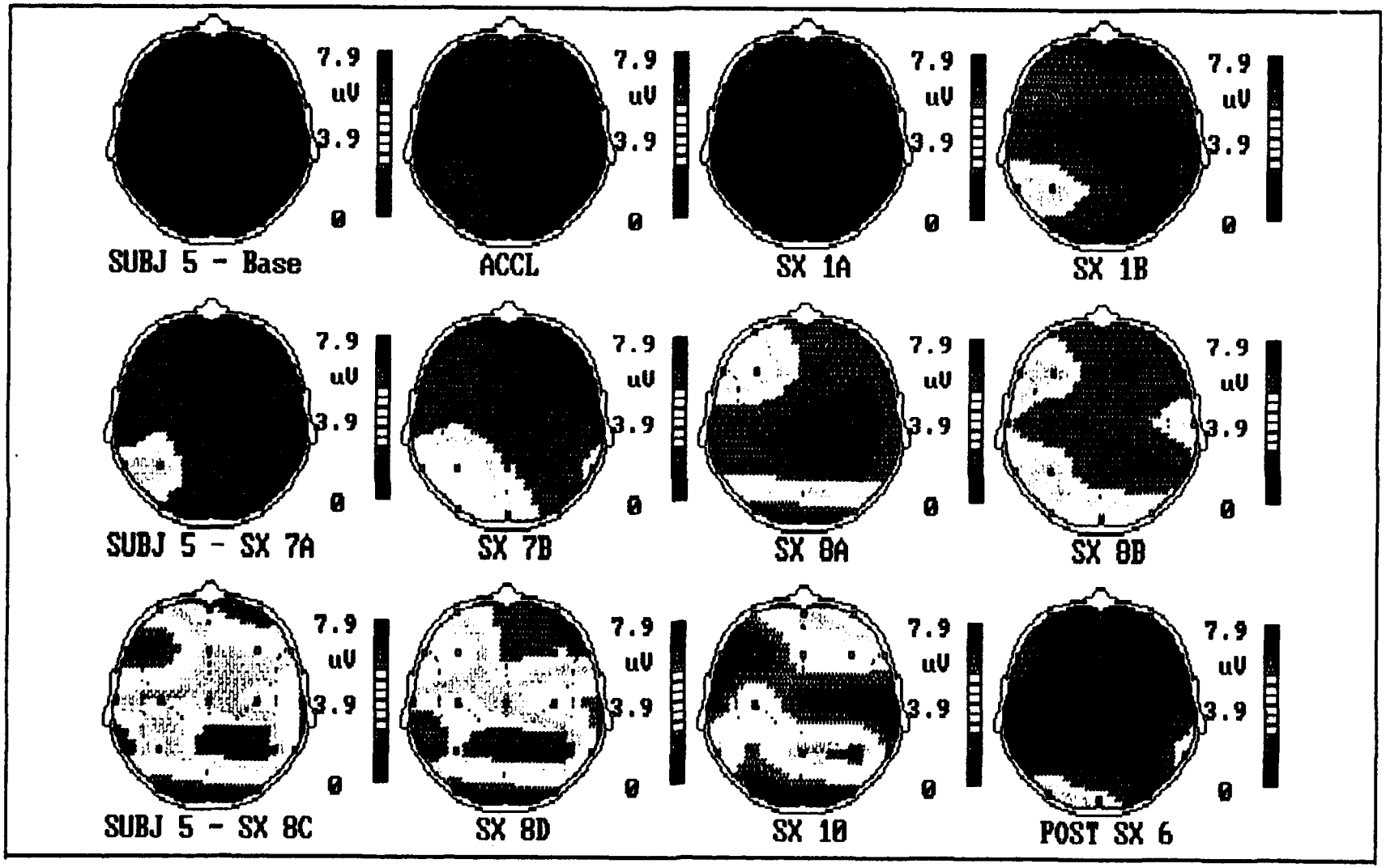

Figure 11. Subject 5 State Maps. Maps are displayed at 1 Hz. Notice how a clear right temporal focus develops.

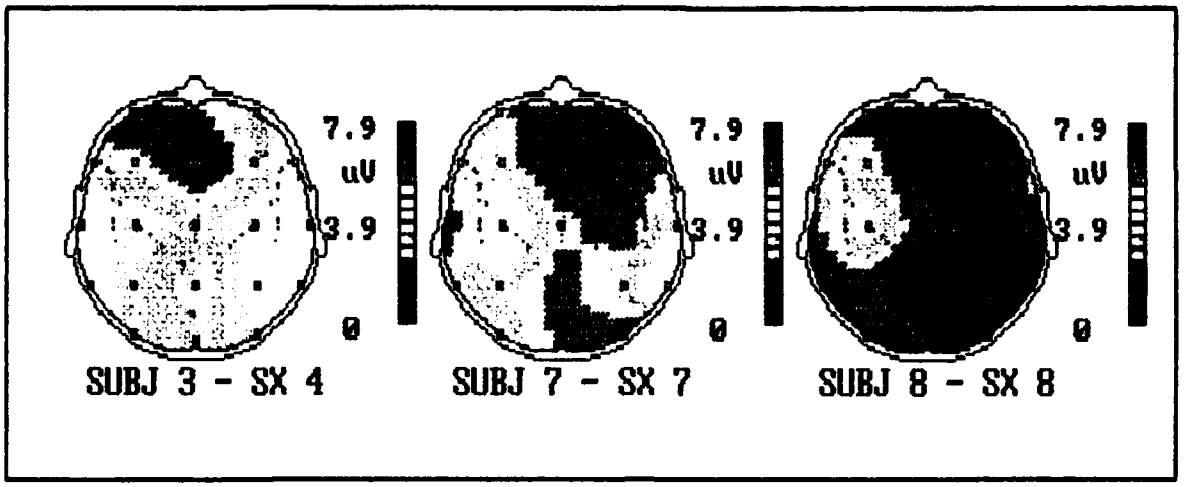

Figure 12. Map Peculiarity. The Brain maps of the three left-handed subjects are shown revealing how the typical parietal and fronto-temporal activity in the left hemisphere has been replaced by more temporal activity.

Finally, before proceeding with the phenytoin trial comparisons, a schematic depicting a generic or ideal progression of high-energy delta activity in the development of motion sickness is shown in Figure 13.

4 Phenytoin Efficacy

Subjects 9 and 11 participated in a 48-hour dosing double-blind placebo vs. phenytoin trials. Based on the time of first head motion to the time of emesis shown in Table 1, Subject 9 performed 96 percent better on phenytoin than placebo, and Subject 11 performed 27 percent worse on phenytoin than placebo. The phenytoin blood level of 11.6 µg/ml in Subject 11 has tended to be ineffective in preventing motion sickness and is the expected reason for his poor performance.

Comparisons of the Subject 9 and 10 brain maps and the Subject 11 and 12 maps offer some interesting results. In both cases the maps of the phenytoin trials appeared to contain less energy than the placebo maps at similar sickness levels. The propagation patterns as described previously did not appear to be affected by the presence of phenytoin. This indicates that phenytoin acts in reducing the magnitude of the electric potentials generated during the development of motion sickness. A

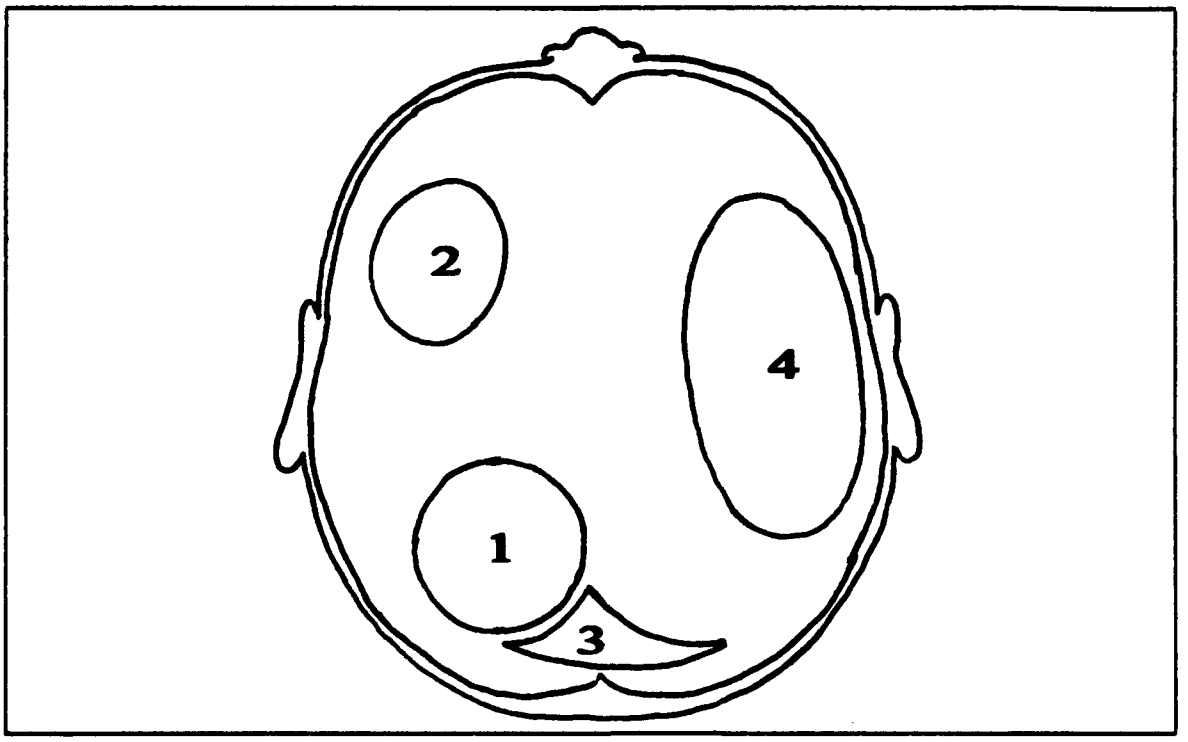

Figure 13. Motion sickness propagation pattern. This schematic shows the probable sequence of events of the EEG changes produced during motion sickness. 1) With initial symptoms, a left parietal focus appears. 2) Almost simultaneously, or shortly thereafter, there is an ipsilateral spread to the fronto-temporal region. 3) A contralateral spread, possibly occipitally, occurs. 4) With more pronounced symptoms a right temporal develops (not always clearly localized). Increased energy is notable throughout the progression.

more important result, perhaps, is that baseline activity while on phenytoin appears to be no different than the baseline activity while on placebo. The state maps of these subjects can be found in Appendix A.

5 Dynamic EEG Results

The dynamic EEG created from the EEG of Subject 5, and recorded on video tape, successfully revealed the development of motion sickness. The foci were readily seen as the severity of symptoms progressed. The overall buildup of energy in the delta band and the waxing and waning nature of all the bands were clearly unveiled. An example of the waxing and waning build in power is shown in Figure 14. Additional dynamic EEGs are displayed in Appendix B.

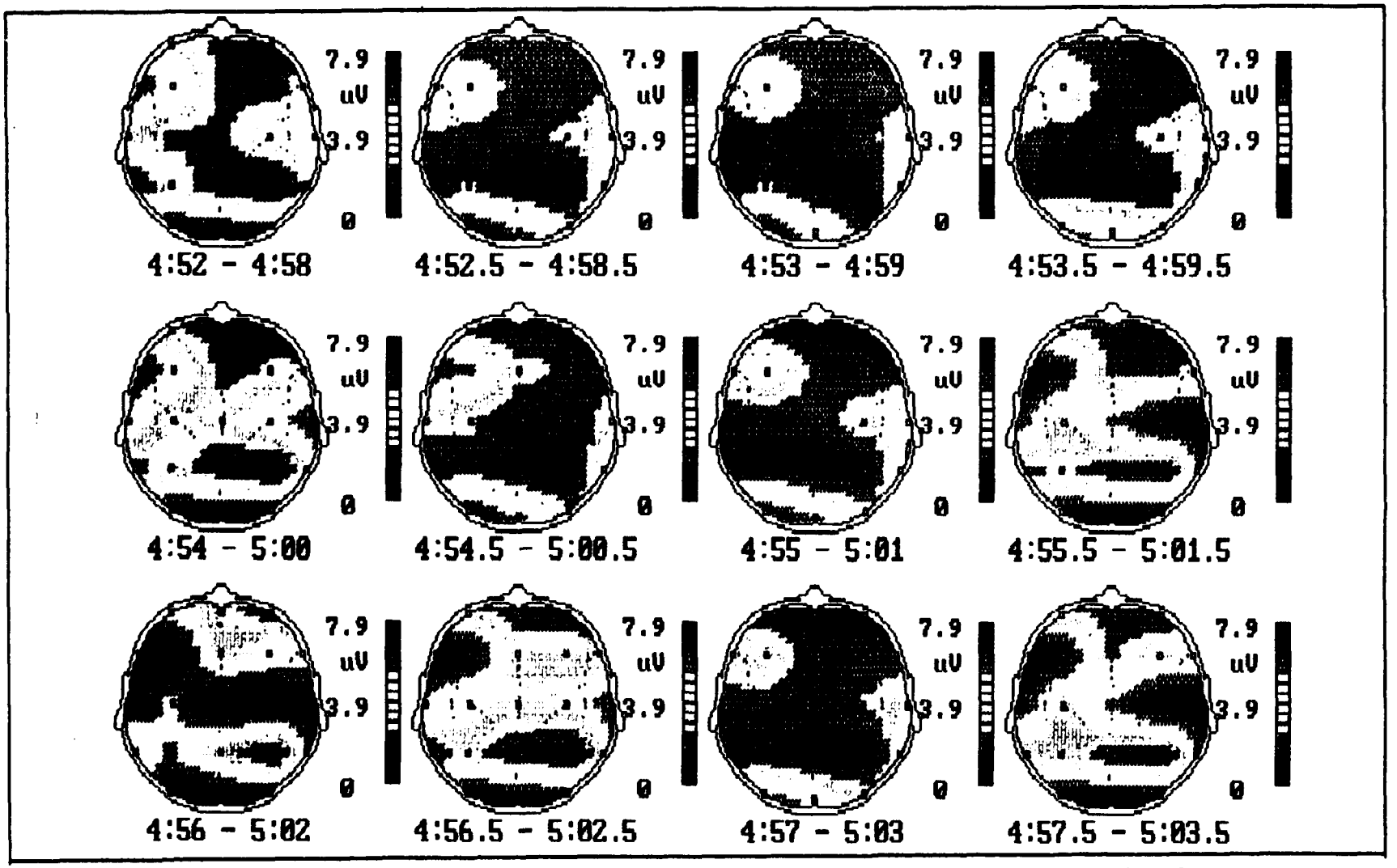

Figure 14. Dynamic Maps. Subject 5 at 1 Hz, level 9 (severe nausea). Note the clear wax and wane as well as a clearly localized temporal focus.

VI Conclusions and Recommendations

1 Conclusions

The most important conclusion drawn from the results expressed in Chapter V is that during the development of motion sickness delta activity dominates and a clear cortical focus establishes spreading ipsilaterally and, then, contralaterally. Although the spatial resolution is limited by the number of electrodes used and the difficulties in making exact placements, the localizations are common to the majority of subjects. In all 12 subjects a left parietal focus was present while 11 of 12 subjects showed a less dominant frontal temporal activity. A bilateral propagation to the right temporal area was observed in 11 subjects as the level of sickness increased. The subject who did not develop a clear increase in right temporal activity ended his trial at the initial nausea level possibly prior to the establishment of increased activity in this area.

The eventual domination of sub-delta activity in the evolution of motion sickness, in addition to a clear focus and spread, adds credence to the possible classification of motion sickness as an ictal or epileptic event as defined by Hughes and Neidemeyer and mentioned in Chapter II (28: 125; 43: 156). The case of motion sickness as a seizure-like or nonepileptic event is left open for the specialized epileptologist and neurologist to resolve after more extensive research is accomplished.

The significant increases of delta and theta activity and the insignificant increases of alpha and beta activity during motion sickness, revealed through this topographic analysis, are consistent with the results obtained by Chelen and the suspicions of Banducci (2: 124; 7). The cortical representation of motion sickness is also supported by much earlier related studies. Mickles and Ades, and Spiegel, using evoked potentials, established a cortical representation of vestibular activity

(47:545). Studies have also shown intense vertigo and the subjective sensation of rotation (common to motion sickness) often occur with stimulation of the parietal lobe, specifically, the superior lip of the interparietal sulcas (38: 161). This agrees with the localization of the initial focus which develops during the earliest stages of motion sickness. The appearance of the less dominant fronto-temporal activity could be explained by the fact that many of the principal afferent (impulse-carrying) fibers to the frontal lobe are from the parietal and occipital regions (38: 401).

Although speculative at this point in time, the increased theta activity noted in rare EEG studies of astronauts or cosmonauts during spaceflight may reveal a definite relationship between space and earth motion sickness. With the intent of monitoring REM sleep patterns during the first several days of spaceflight (when space sickness occurs) the EEGs of cosmonaut P. R. Popovich and astronaut Frank Borman revealed increased theta activity (1; 43: 462). Particularly interesting in the case of Frank Borman's Gemini 7 flight was that the theta activity was detected in the parieto-occipital leads of the left hemisphere (1). The similarity with the increased theta activity associated with the high-energy delta activity during motion sickness is interesting, although far from conclusive.

Unfortunately, despite palpable signs of the cortical representation and propagation of motion sickness, the results offer no clear indications of the subcortical activity and latencies involved with Coriolis stimulation and the evolution of motion sickness. Are the foci demonstrated in the development of motion sickness synaptically connected to one another or are they produced by underlying subcortical activity? The development of the fronto-temporal focus could be explained by the constant firing of the more dominant parietal focus ipsilaterally (28: 126). The apparent occipital bilateral propagation revealed by the brain maps suggests the involvement of the corpus callosum if the spread of cortical

activity from left to right is directly related. The complex relationship between the cerebellum and the vestibular, visual, visceral, and reticular systems combined with the two-dimensional limitation of the topographic map makes it extremely difficult to determine the cause of the cortical activity, let alone determine whether the increased activity is due to synaptic excitation or inhibition, or seizure activity (43: 340; 47: 545-6; 49: 241). The occasional appearances of increased bilateral frontal lobe activity, although not appearing to be artifactual, may be due to an increased effect of the vestibular system on the extraocular muscles during more severe stages of motion sickness (47: 546).

Although much remains to be answered as to why the patterns seen during motion sickness exist, the fact remains that they do exist. As a result, studies of how motion sickness treatments effect or relate to this pattern are important and may permit the predictions of how a subject will respond to a drug (35: 174). The clear presence of more high-energy activity in placebo-treated subjects than in the respective phenytoin-treated subjects suggests that phenytoin does act to reduce the EEG activity during the evolution of motion sickness. The results also indicate that the overall propagation pattern does not change. The key to determining the efficacy of phenytoin and to finding the EEG activity which triggers an emetic response lies in the EEGs of subjects who do not get sick from excessive motion stimulation. If, for example, there is no bilateral propagation or insignificant bilateral propagation for a subject who remains asymptomatic while on phenytoin, questions as to its efficacy and the cortical precursor to a vomiting episode may be answered. At this point, the brain maps suggest a emetic response results when the threshold of stimulation (possibly in the right temporal region) an individual can withstand is exceeded. This conclusion results from the overall build in power seen clearly in dynamic maps.

The dynamic map, especially in the video version, is definitely an aid in identifying patterns in motion sickness. Dynamic mapping in the subjects examined clearly shows the waxing and waning nature of the EEG and the corresponding increase in energy as symptoms worsen. As a communicative device, the dynamic map appears to be much more valuable than the state maps. The large amount of time required to create and film the individual files is a major drawback, however.

2 Recommendations

The results of this thesis warrant continued research in the use of phenytoin or other anticonvulsant drugs in preventing motion sickness. Future research should include controlled, operational lab and EEG studies. In particular, future EEG studies should investigate the ability of phenytoin to reduce the spread of activity from the parietal lobe and to limit the power which increases during motion sickness. Being the first known report of such a pattern, a larger number of subjects should be examined for such a pattern and, once a large enough database is built, a statistical approach may be tried. If possible, an attempt to use some sort of evoked-potential technique to determine the latencies produced by Coriolis stimulation and how they relate to the reported foci might prove interesting.

The existence of a propagation pattern during motion sickness stimulates several ideas. The first, is to encourage epileptologists and neurologists to take interest in the similarities of motion sickness to simple partial seizure and to apply their specialized experiences in studying this age old malady. Second, a three-dimensional look at the brain would provide some interesting answers to the cortical and subcortical representation of motion sickness. A current interest in attempting to use Positron Emission Tomography (PET) offers promise in this area if an adequate means of instilling motion sickness and at the same time utilizing PET facilities is

determined. A recent PET identification of the human visual motion area (V5) in the prestriate cortex near the temporal and occipital lobe junction shows the usefulness of PET and is thought provoking if one considers the existence of a relationship between other motion-influenced areas (58: 186).

A third idea stems from the large degree of user interaction required in using the Brain Atlas to analyze anything but 2-second epoches. The 10-second and 6-second FFTs were useful but slow to produce. Even larger epoches may be desired to better represent a state or level of motion sickness. Larger epoches would, in effect, average in the extrema which result from waxing and waning patterns. A study of larger epoches could be accomplished in a variety of ways. First, standard use of the Brain Atlas can be continued. Second, more capable software such as Codas and Asystant could be used to digitize analog EEG, perform a spectral analysis, and then convert this information into files the Brain Atlas can spatially display. The third approach moves away from use of the Brain Atlas and applies the use of an artificial neural network.

Based on the areas of cortical localization defined in this thesis, one or two channels from each area can be used to provide features (amplitude, absolute power, relative power) sampled from various sickness levels of a group of subjects. These features could then be input into a feedforward, back-propagation, or clustering network as desired and the results used to determine if stages of motion sickness are discernable. The question of how to normalize the data would have to be resolved, although the transformation used by John, as discussed in Chapter III, might be useful. Siguenza *et al* have recently shown such an approach is reliable in classifying visually-evoked potentials of rats (52).

The final recommendation concerns the dynamic EEG. Additional dynamic EEGs need to be created possibly using more professional equipment. Efforts in

finding a way to continuously display a variety of maps using a range of epoch sizes should be made for two reasons. First, it could provide a more efficient means of analysis. Second, and maybe most important to the future of this line of motion sickness research, is that the dynamic EEG, as an animation, can sell the importance of this research and hopefully convince people of the results in several minutes without the need for elaborate explanations which could be required with a series of single maps.

Appendix A

State Maps

The maps displayed in Appendix A are the state maps of the 10 subjects whose maps were not presented in Chapter V. The maps are read from left to right with the sickness level designation under each map. In those cases where the designation POST is used, it refers to data analyzed after Sickness Level 10 vomiting or wretching, revealing the subject's state at the specified sickness level. Each of the state maps is of a specific amplitude in the delta band (1 or 1.5 Hz) and is representative of the maps obtained from looking at the 0.5 - 3.0 delta band.

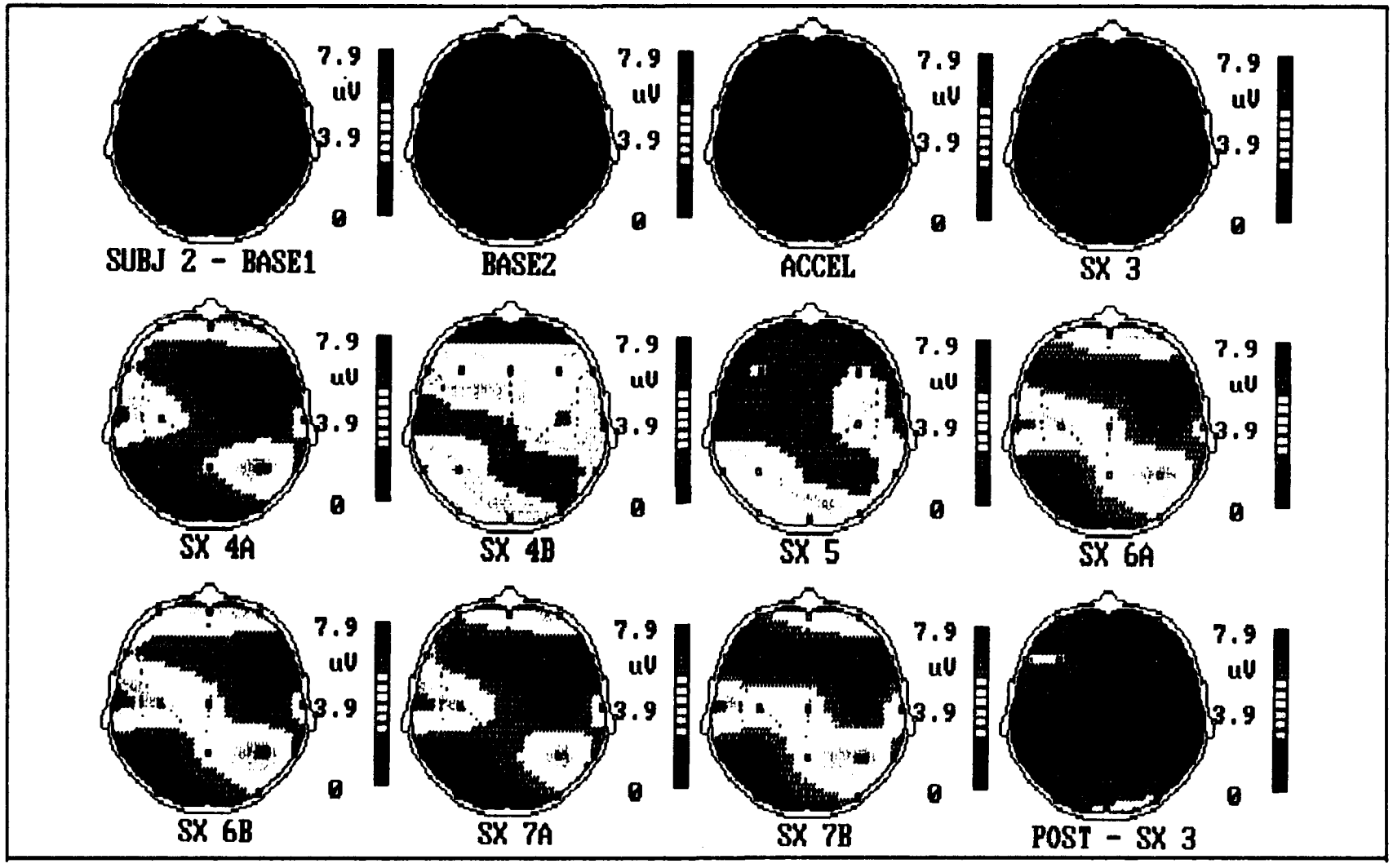

Subject 2 state maps displayed at 1 Hz. Notice how high power appears as early as Sickness Level 4

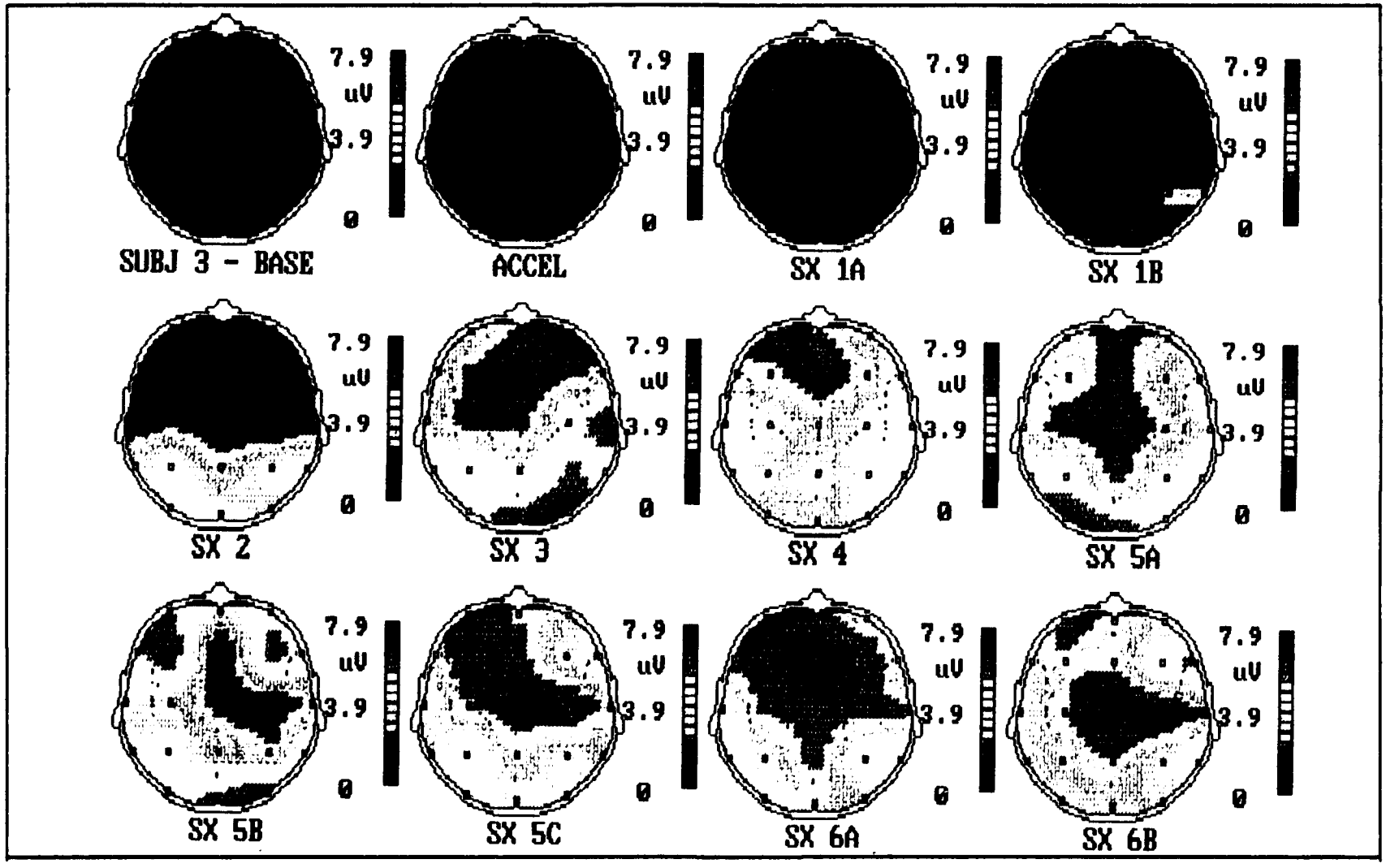

Subject 3 state maps displayed at 1 Hz. Notice the lack of a clear focus in the right temporal region or of any significant left fronto-temporal activity.

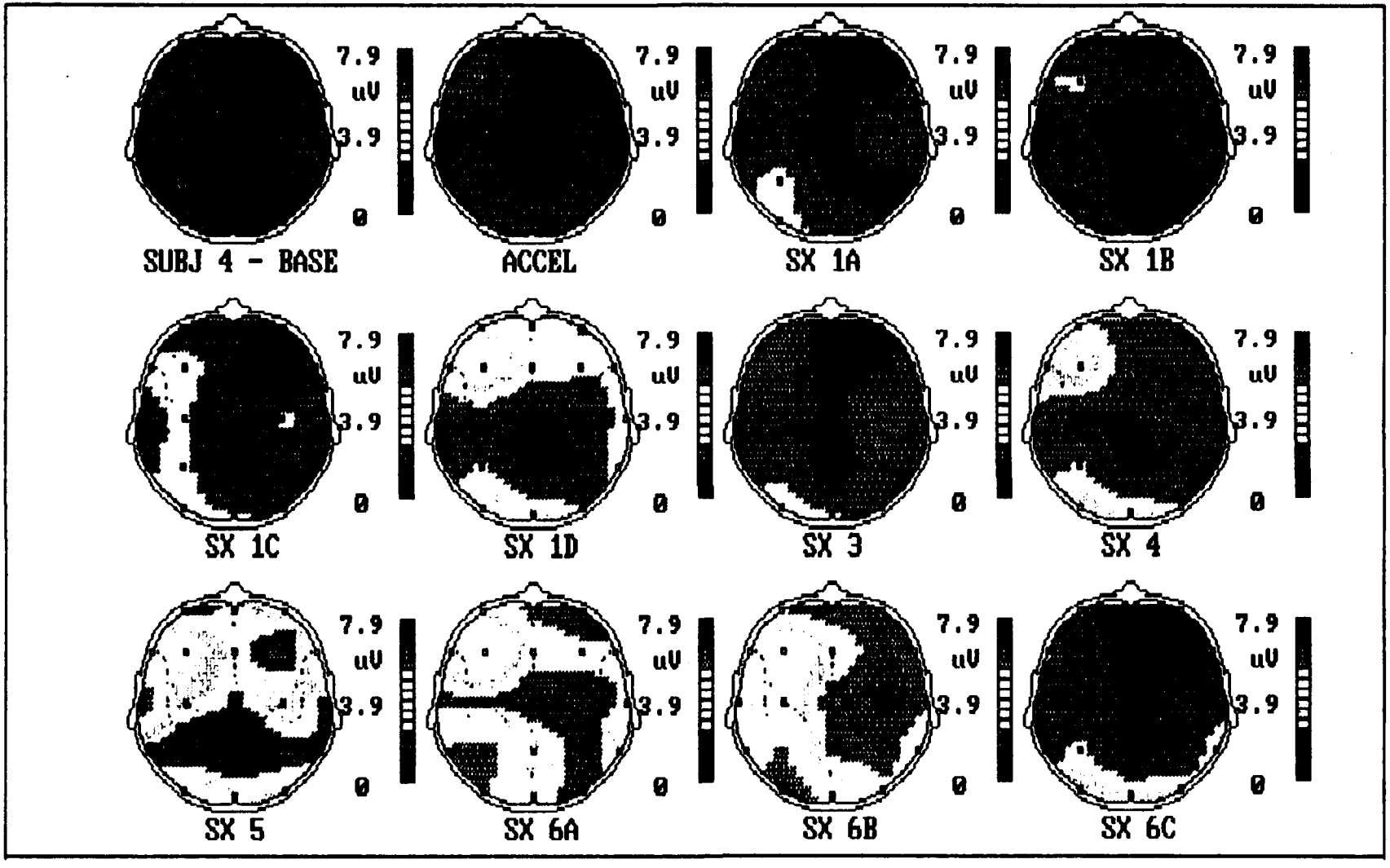

Subject 4 state maps displayed at 1 Hz. Note how a right temporal focus has not developed. This may be because this subject's trial was ended at initial nausea (SX 6).

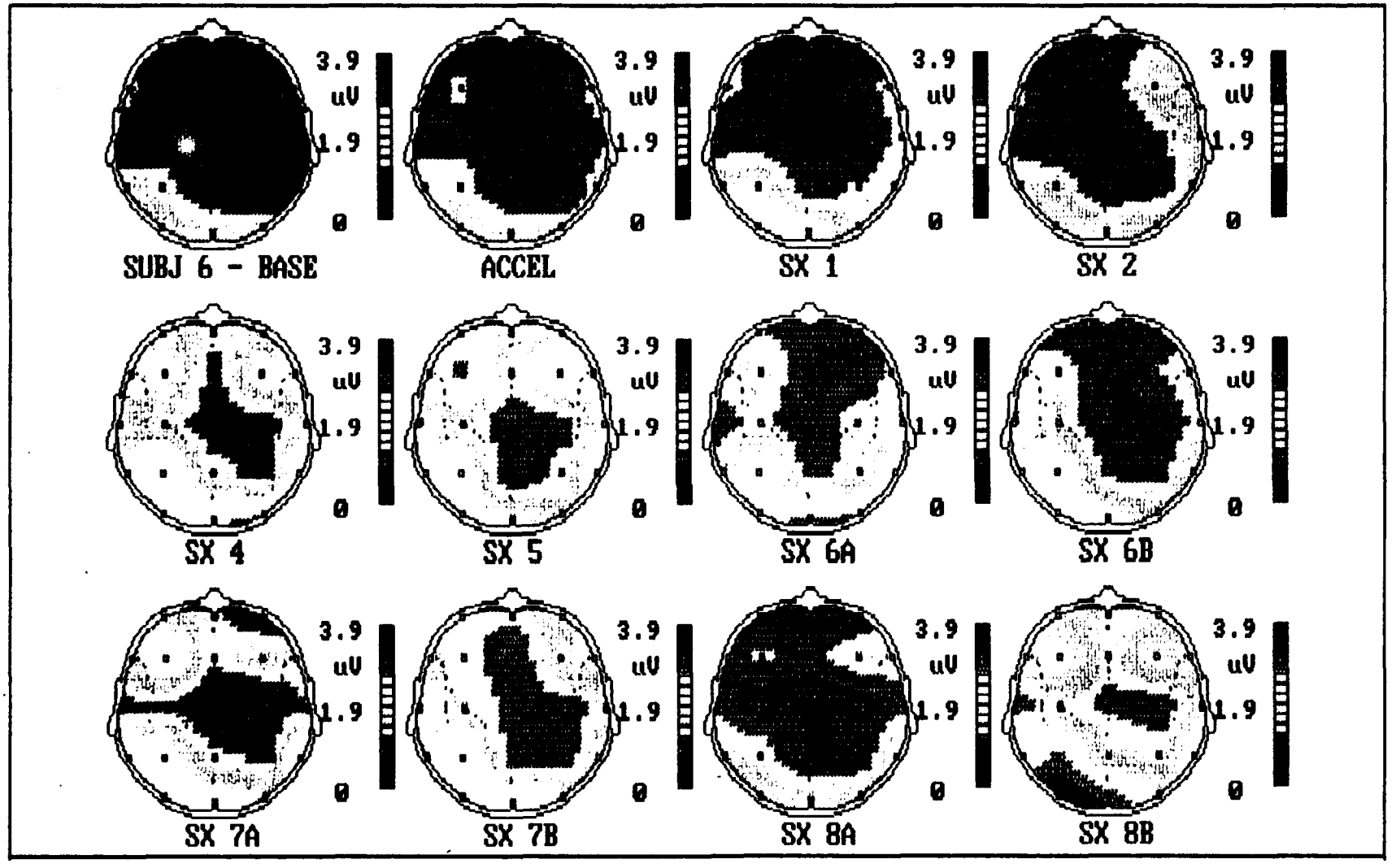

Subject 6 state maps displayed at 1.5 Hz. A clearly localized right temporal focus is not seen. Notice that compared to other subjects less energy developed in this female subject .

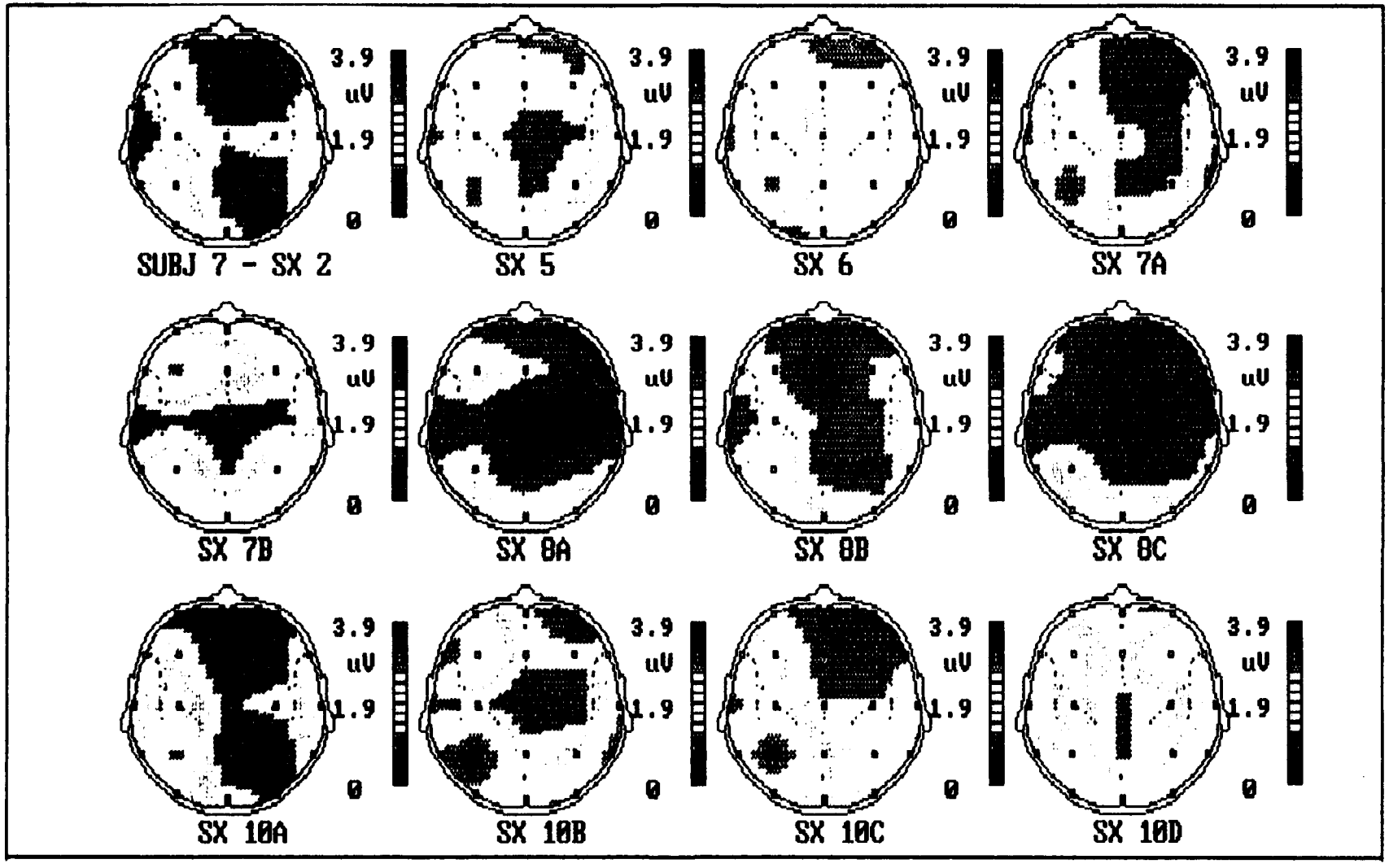

Subject 7 state maps. Maps are displayed at 1.5 Hz. Baseline data was not available. This female subject also shows less power was needed for effects similar to the others.

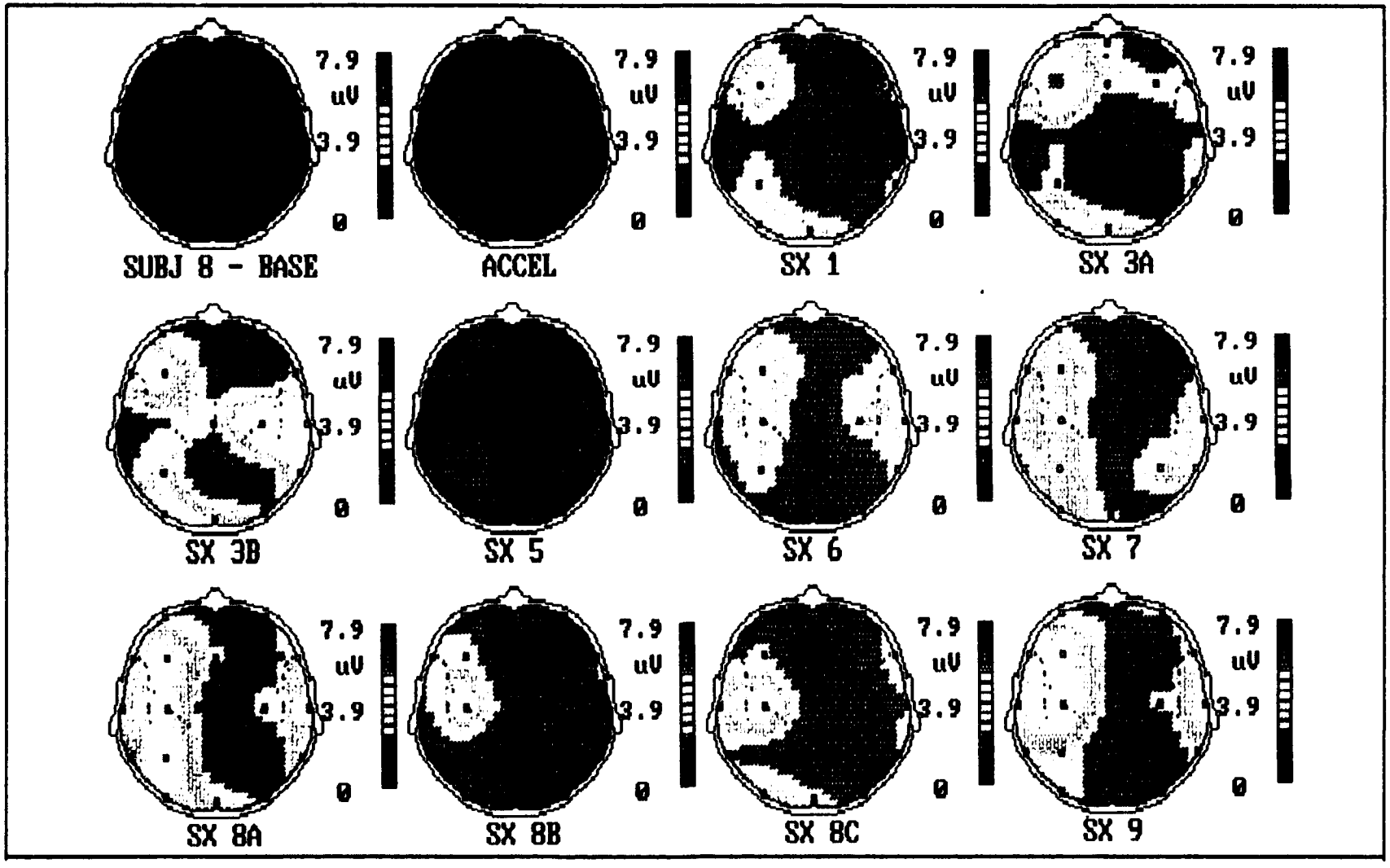

Subject 8 state maps at 1.5 Hz. The maps of the third female subject were also less energetic. Note the occurrence of a shift to left temporal activity.

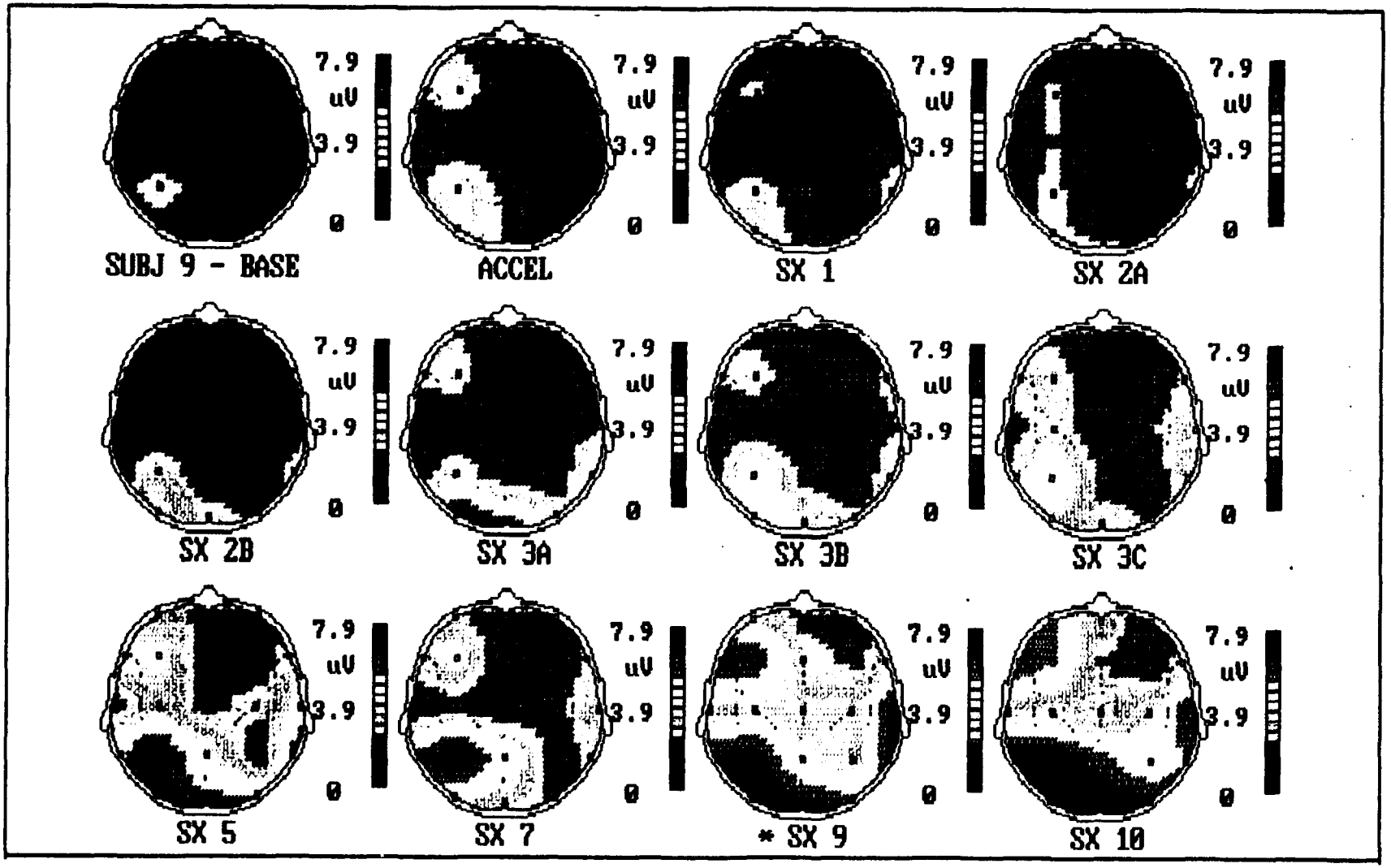

Subject 9 state maps displayed at 1 Hz. A clear progression is seen here. This subject was treated with phenytoin. A comparison can be made with Subject 10.

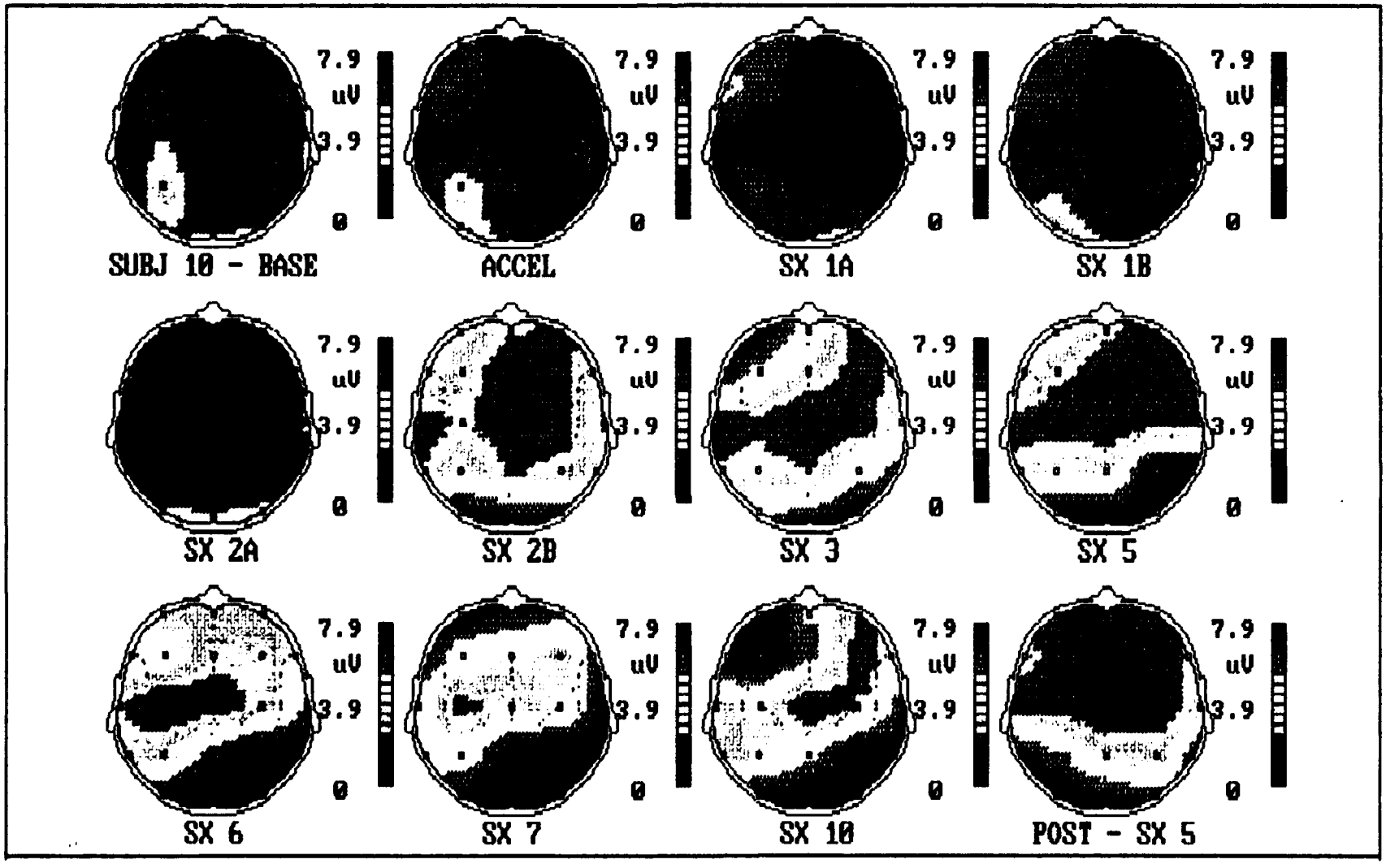

Subject 10 state maps displayed at 1 Hz. Notice the lack of a clear focus in the right temporal region. More power appears during this placebo trial compared to Subject 9

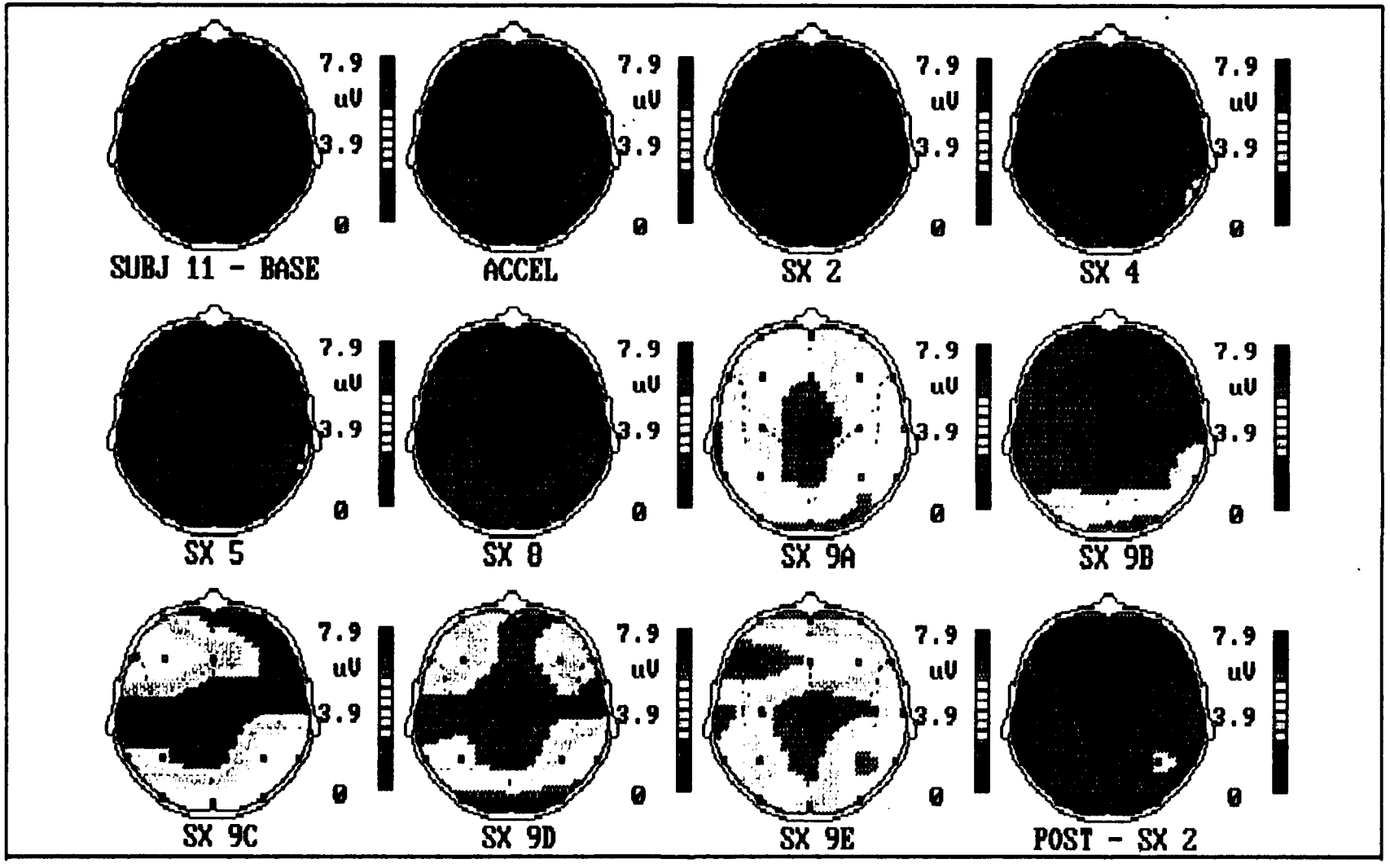

Subject 11 state maps at 1 Hz. No clearly localized right temporal focus is apparent in this phenytoin treated subject. Less overall power is noticeble compared to Subject 12.

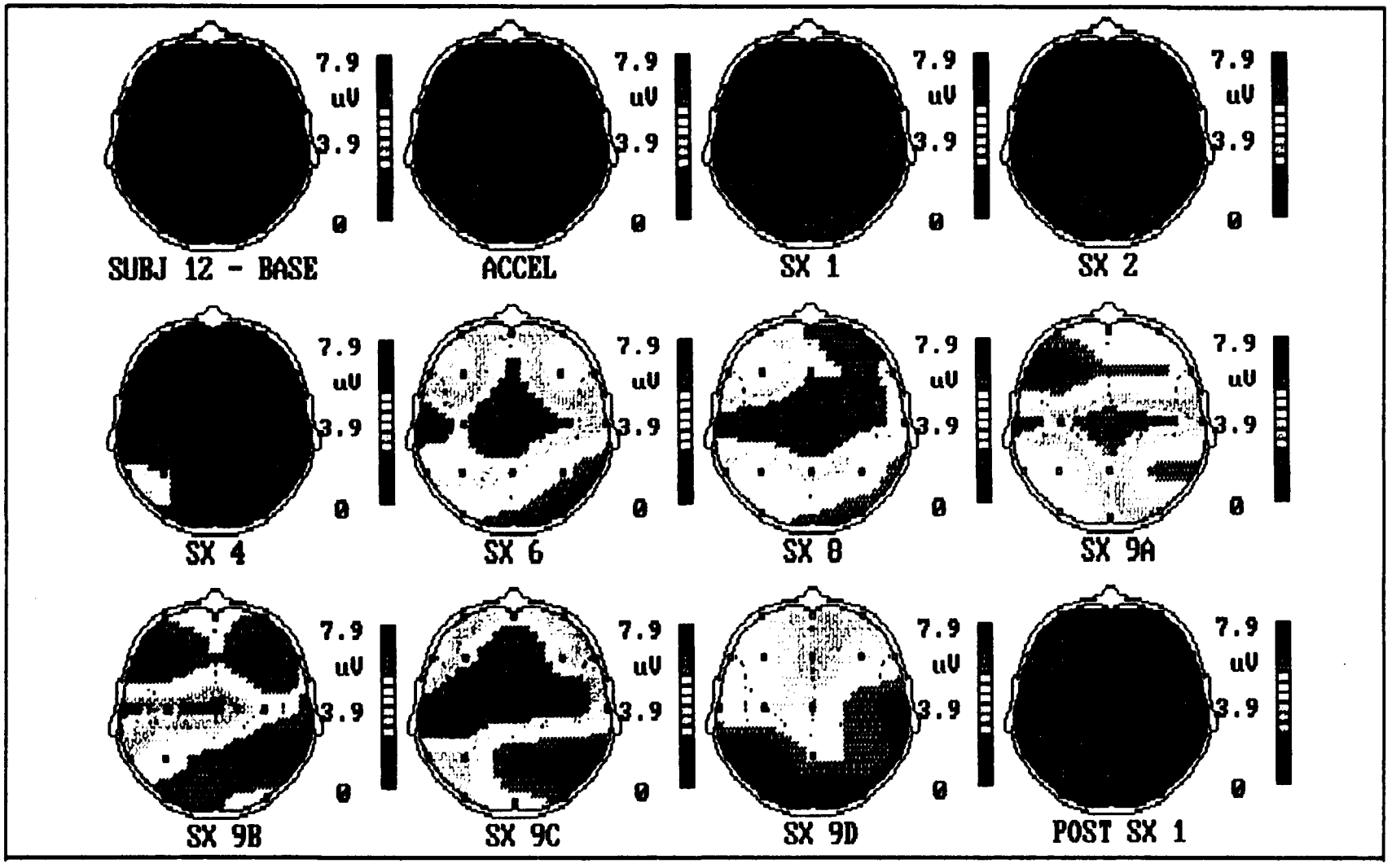

Subject 12 state maps at 1 Hz. More energy is apparent in this placebo trial as compared to Subject 11. Waxing and waning is noticeble and no clearly localized focus is present.

Appendix B

Dynamic Maps

The four dynamic maps presented in this appendix are read from left to right. Each map was obtained from a fast Fourier transform of the 6-second period indicated. The maps are of a specific frequency (1 or 1.5 Hz) of the delta band. Each map is representative of the maps of the 0.5 - 3.0 Hz delta band. Each map is shifted 0.5 seconds in time, therefore, a total of 11.5 seconds is shown during the sickness level designated by the subject. All times referenced are in minutes and seconds.

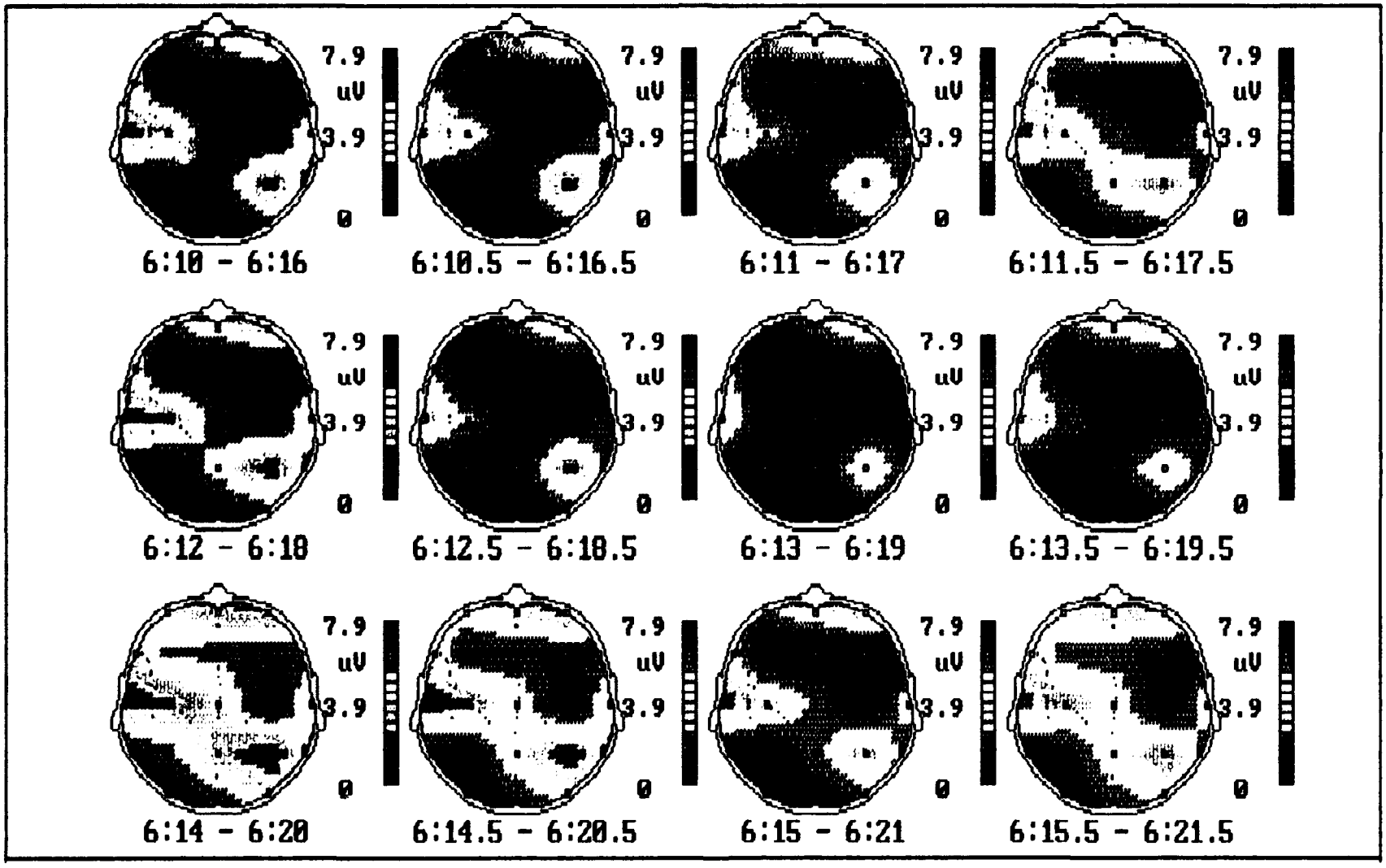

Subject 2 dynamic maps at 1 Hz. Subject reports a Sickness Level 6 but reaches emesis at approximately 6:36. Head motions had been stopped at this time.

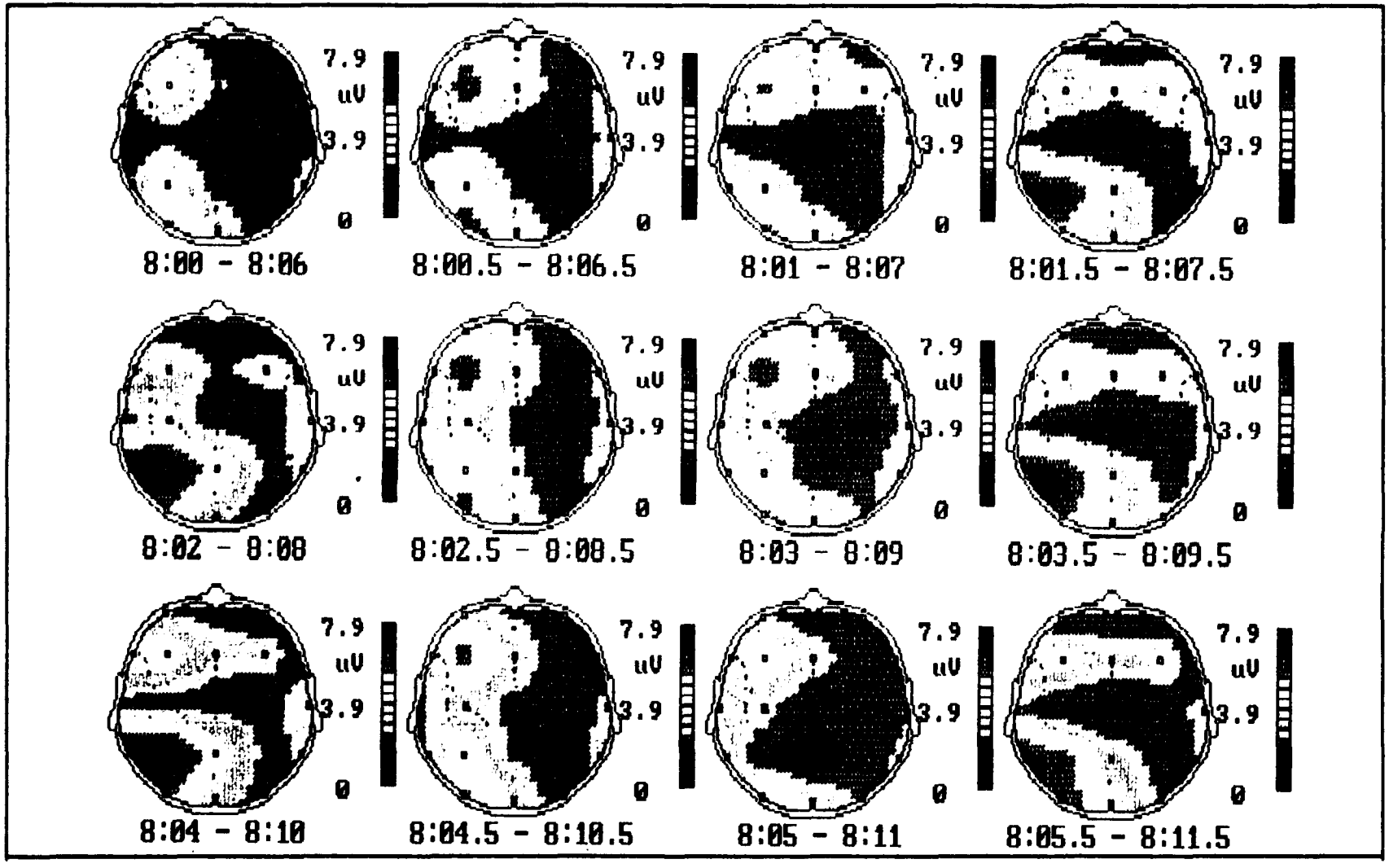

Subject 4 dynamic maps at 1 Hz. Subject reports Sickness Level 6 (nausea). Left hemisphere activity is well developed and there are signs of right temporal activity.

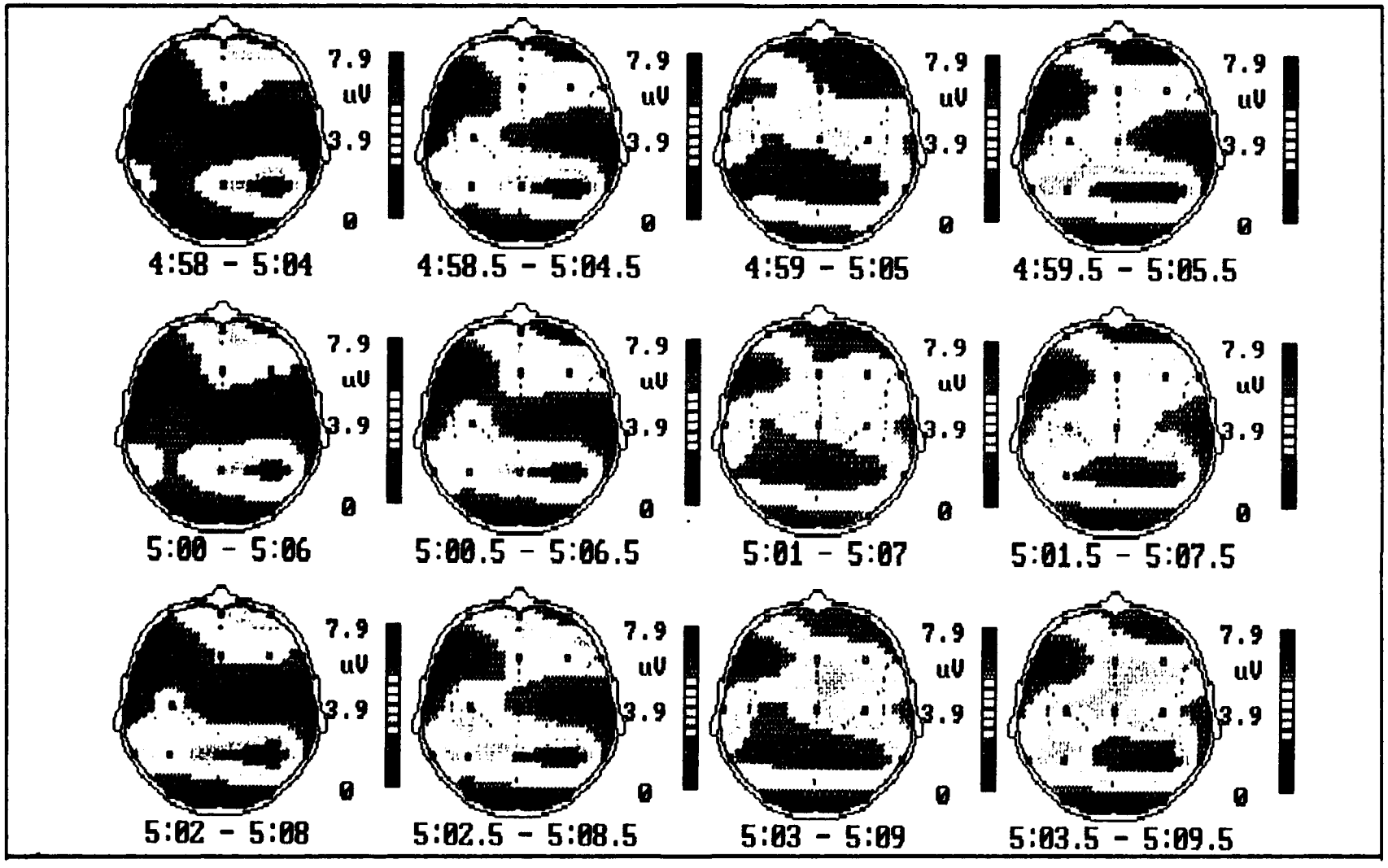

Subject 5 dynamic maps at 1.5 Hz. A continuation of the maps shown in Figure 14 (p. 48). At Sickness Level 9, with no head motions, a definite rhythm is noticeable.

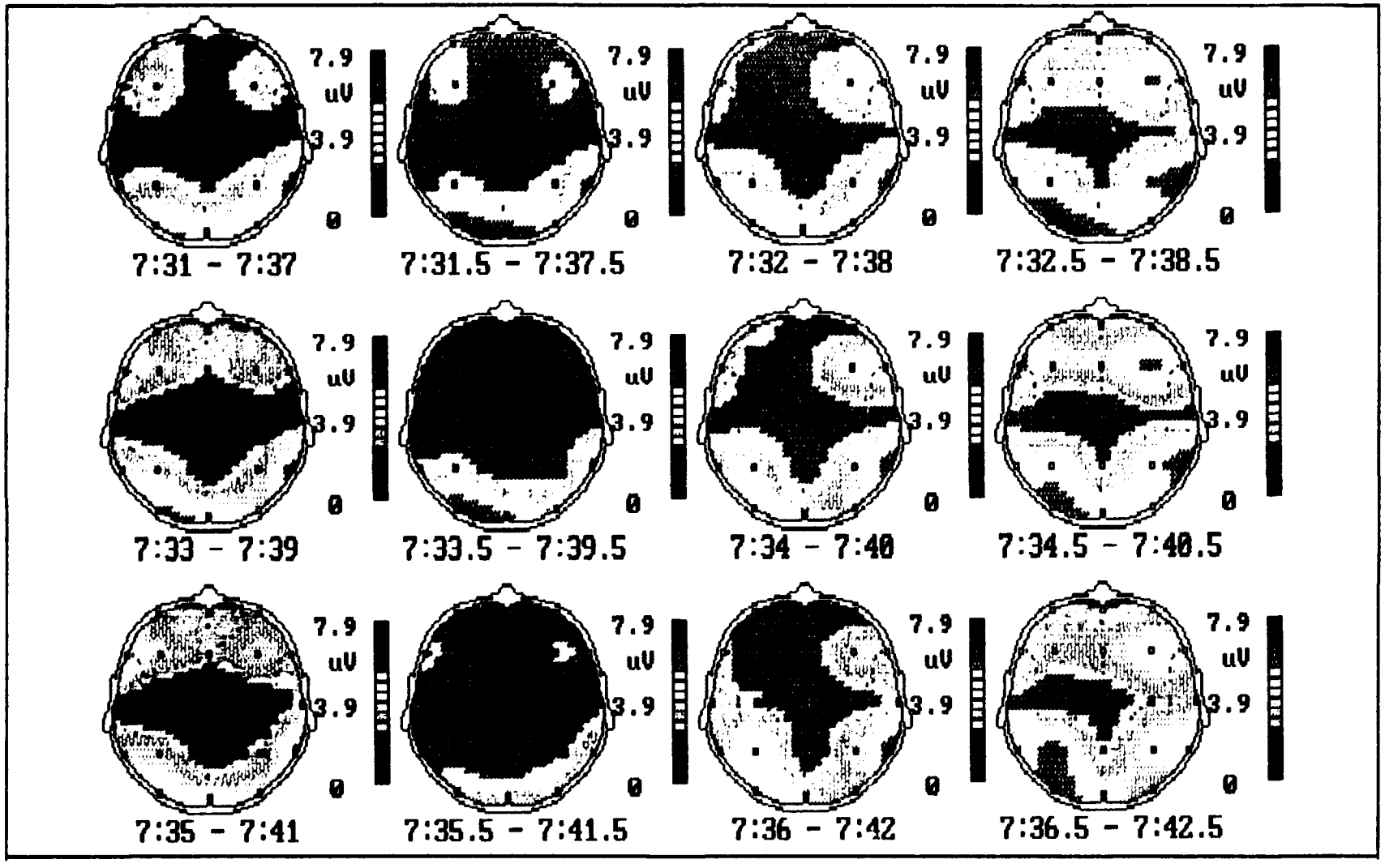

Subject 12 dynamic maps at 1.5 Hz. At Sickness Level 9.5 (severe nausea) more right fronto-temporal activity than normal is seen. Emesis reached 3 min 40 sec later.

Bibliography

1. Adey, W. R. et al. "Computer Analysis of EEG Data from Gemini Flight GT-7," Aerospace Medicine, 38: 345-359 (April 1967).

2. Banducci, Capt Todd M. An Analysis of the Effects of Phenytoin in Treating Motion Sickness and the Effects of Motion Sickness on the Human Electroencephalogram. MS thesis, AFIT/GSO/ENG/90D-2. School of Engineering, Air Force Institute of Technology (AU), Wright-Patterson AFB OH, Dec 1990.

3. Bock, Otmar L. and Charles M. Oman. "Dynamics of Subjective Discomfort in Motion Sickness as Measured with a Magnitude Estimation Method," Aviation, Space, and Environmental Medicine, 53(8): 773-777 (August 1982).

4. Booker, Harold E. et al. "Effects of Diphenylhydantoin on Selected Physiological Measures in Normal Adults," Neurology, 17: 949-951 (October 1967).

5. Chelen, William E. Test Plan for Laboratory and Field Evaluation of the Therapeutic Efficacy of Phenytoin Upon Motion Sickness. Harry G. Armstrong Aerospace Medical Research Laboratory & Air Force Institute of Technology: Wright Patterson AFB, OH (15 Feb 1991).

6. Chelen, William E. et al. "Use of Phenytoin in the Prevention of Motion Sickness," Aviation, Space, and Environmental Medicine, 61: 1022-5 (November 1990).

7. Chelen, William E. et al. "Spectral Analysis of the Electroencephalographic Response to Motion Sickness." Draft of Report Submittal. Air Force Institute of Technology, and Armstrong Aerospace Medical Laboratory, Wright-Patterson AFB, Dayton OH, May 1991.

8. Cohen, Leonardo G. and Mark Hallett. "Noninvasive Mapping of Human Motor Cortex," Neurology, 38: 904-909 (June 1988).

9. Davis, Jeffrey R. et al. "Space Motion Sickness During 24 Flights of the Space Shuttle," Aviation, Space, and Environmental Medicine, 59: 1185-89 (December 1988).

10. Davis, Jeffrey R., and B. Beck. "Update on the Incidence of Space Motion Sickness," Aerospace Medical Association 61st Annual Scientific Meeting. New Orleans, LA, May, 1990.

11. Devinsky, Orrin et al. "Clinical and Electroencephalographic Features of Simple Partial Seizures," Neurology, 38: 1347-52 (September 1988).

12. Dhenin, G. "Motion Sickness," Aviation Medicine, Chapter 22. London: Tri-Med Books Limited, 1978.

13. Dreifus, F. E.. "A Classification of Epileptic Seizures and the Epilepsies," Advances in Epileptology: XIIIth Epilepsy International Symposium, edited by H. Akimoto et al. New York: Raven Press, 1982.

14. Duffy, Frank H. et al. "Significance Probability Mapping: an Aid in the Topographic Analysis of Brain Electrical Activity," Electroencephalography and Clinical Neurophysiology, 51: 455-462 (1981).

15. Fisch, Bruce J. et al. "A Topographic Background Symmetry Display for Comparison with Routine EEG," Electroencephalography and Clinical Neurophysiology, 69: 491-494 (1988)

16. Fix, Capt Edward L. Motion Sickness: Quantitative Algorithmic Malaise Indication in Real Time. MS Thesis, AFIT/GE/ENG/87D-18. School of Engineering, Air Force Institute of Technology (AU), Wright-Patterson AFB OH, December 1987 (AD-A189674).

17. Fox, Shaul and Isaac Aaron. "Motion Sickness and Anxiety," Aviation, Space, and Environmental Medicine 59: 728-33 (August 1988).

18. Gale, Karen. "Progression and Generalization of Seizure Discharge: Anatomical and Neurochemical Substrates," Epilepsia, 29(Suppl 2): S15-S34 (1988).

19. Gasser, Theo et al. "Transformations Towards the Normal Distribution of Broad Band Spectral Parameters of the EEG," Electroencephalography and Clinical Neurophysiology, 53: 119-124 (1982).

20. Giard, M. H. et al. "Several Attention-Related Wave Forms in Auditory Areas: A Topographic Study," Electroencephalography and Clinical Neurophysiology, 69: 371-384 (1988).

21. Gray, Henry. Gray's Anatomy, edited by T. Pickering Pick, Philadelphia: Running Press (1974).

22. Gregory, D.L. and P.K. Wong. "Topographical Analysis of the Centrotemporal Discharges in Benign Rolandic Epilepsy of Childhood," Epilepsia, 25(6): 705-711 (1984).

23. Griffith, H. Winter. Complete Guide to Prescription & Non-Prescription Drugs. New York: Body Press/Perigee (1991).

24. Guenther, William. et al. "EEG Mapping of Left Hemisphere Dysfunction During Motor Performance in Schizophrenia," Biological Psychiatry, 21: 249-62 (1986).

25. Guyton, A.C. Textbook of Medical Physiology. Philadelphia: W.B. Saunders Company, 1971.

26. Guyton, A.C. Textbook of Medical Physiology. Philadelphia: W.B. Saunders Company, 1991.

27. Homick, J. L. et al. "Space Adaptation Syndrome: Incidence and Operational Implications for the Space Transportation System Program," Advisory Group for Aerospace Research and Development (AGARD) Conference Proceedings No. 372 (November 1984).

28. Hughes, John R. EEG in Clinical Practice. Boston: Butterworths Publishers Inc., 1982.

29. Isaksson, Anders et al. "Computer Analysis of EEG Signals with Parametric Models," Proceedings of the IEEE, vol. 69, No. 4: 451-461. New York: IEEE Press, April 1981.

30. John, E.R. et al. "Developmental Equations for the Electroencephalogram," Science, 210: 1255-8 (12 December 1980).

31. John, E.R. et al. "Neurometrics: Computer-Assisted Differential Diagnosis of Brain Dysfunctions," Science, 239: 162-169 (8 January 1988).

32. Jones, David R. et al. "Self-Control of Psychophysiologic Response to Motion Stress: Using Biofeedback to Treat Airsickness," Aviation, Space, and Environmental Medicine, 56: 1152-7 (December 1987).

33. Jonkman, J. et al. "The Use of Neurometrics in the Study of Patients with Cerebral Ischaemia," Electroencephalography and Clinical Neurophysiology, 61: 333-341 (1985).

34. Joyce, Christopher. "Space Travel is No Joyride," Psychology Today, 18: 30-37 (May 1984).

35. Kahn, E. Michael et al. "Topographic Maps of Brain Electrical Activity -- Pitfalls and Precautions," Bioloical Psyciatry, 23: 628-636 (1988).

36. Kanazawa, Osamu et al. "Dynamic EEG Topography in Epileptic Siezures," The Japanese Journal of Psychiatry and Neurology, 43(3): 544-545 (September 1989).

37. Karkishchenko N. N. and N. A. Dimitriadi. "Anticonvulsants as Protective Agents in Space Motion Sickness," Kosmicheskaya Biologiya i Aviakosmicheskaya Meditsina, 29: 1351, 1990. Translation of Published Abstract, Neurophysiology: 92 (1990).

38. Krieg, Wendell J. S. Functional Neuroanatomy. New York: The Blakiston Company, Inc., 1953.

39. Llinas, Rodolfo R. The Biology of the Brain From Neurons to Networks. New York: W.H. Freeman and Company, 1988.

40. Lombroso, C.T. and F.H. Duffy. "Brain Electrical Activity Mapping in the Epilepsies," Advances in Epileptology: XIIIth Epilepsy International Symposium, edited by H. Akimoto et al. New York: Raven Press, 1982.

41. Lopes da Silva, F.H. "A Critical Review of the Clinical Applications of Topographic Mapping of Brain Potentials," Journal of Clinical Neurophysiology, 7(4): 535-51 (1990).

42. Lukas, Scott E. "Topographic Distribution of EEG Alpha Activity During Ethanol-Induced Intoxication in Women," Journal of Studies on Alcohol, 50(2): 176-85 (March 1989).

43. Niedermeyer, Ernest and Fernando Lopes da Silva. Electroencephalography. Baltimore--Munich: Urban & Schwarzenberg, 1983.

44. Nuwer, Marc R.. "A Comparison of the Analyses of EEC and Evoked Potentials Using Colored Bars in Place of Colored Heads," Electroencephalography and Clinical Neurophysiology, 61: 310-313 (1985).

45. Nuwer, Marc R.. "Frequency Analysis and Topographic Mapping of EEG and Evoked Potentials in Epilepsy," Electroencephalography and Clinical Neurophysiology, 69: 118-126 (1988).

46. Nuwer, Marc R. "EEG Topographic Mapping and Frequency Analysis: Techniques and Studies in Clinical Setting," Seminars in Neurology, 10(2): 166-177 (June 1990).

47. Parker, James F. Jr. and Vita R. West. Bioastronautics Data Book. Washington D.C.: National Aeronautics and Space Administration, 1973.

48. Rall, Theodore W. and Leonard S. Schleifer. "Drugs Effective in the Therapy of the Epilepsies," The Pharmacological Basis of Therapeutics (6th Edition), edited by Louis S. Goodman. New York: Macmillan Publishing Company, 1980.

49. Reason, J.T. and J.J. Brand. Motion Sickness. London: Academic Press, 1975.

50. Restak, Richard. The Brain. New York: Bantam Books, 1984.

51. Restak, Richard M. The Mind. New York: Bantam Books, 1988.

52. Siquenza, Juan A. et al. "Automatic Classification of Visual Evoked Potentials by Feedforward Neural Networks," Artificial Neural Networks Vol. II. Proceedings of the 1991 Inuternational Conference on Artificial Neural Networks (ICANN-91), Espoo, Finland, 24-28 June 1991. Edited by T. Kohonen et al., North-Holland: Elsevier Science Publishers (1991).

53. Spehlmann R. EEG Primer. Amsterdam: Elsevier Biomedical Press, 1987.

54. Stern, Robert M. et al. "Adaptation to Vection-Induced Symptoms of Motion Sickness," Aviation, Space, and Environmental Medicine, 60: 566-72 (June 1989).

55. Takahashi, Hiroshi et al. "Dynamic EEG Topography and Analysis of Epileptic Spikes and Evoked Potentials Following Thalamic Stimulation," Applied Neurophysiology, 48: 418-422 (1985).

56. Walter, Grey W. and H. W. Shipton, "A New Toposcopic Display System," Electroencephalography and Clinical Neurophysiology, 3: 281-292 (1951).

57. Walter, Grey W. "The Electrical Activity of the Brain," Scientific American: 2-9 (June 1954).

58. Watson, J.D.G. et al. "Identification of the Visual Motion Area (V5) in Humans," Neurology, 41 (Suppl 1): 186 (March 1991).